EXPERIMENTAL PROCEDURES

Reagents and Antibodies—Recombinant human Ang1 was purchased from R&D Systems. In Western blot analysis, mouse anti-phosphotyrosine (4G10) and anti-Tie2 (Ab33) antibodies (Abs) (Upstate), anti-HA.11 mAb (COVANCE), anti-c-Myc (9E10) and Tie1 (C-18) mAbs (Santa Cruz Biotechnology, Inc.), anti-HA-tag rabbit serum (Medical & Biological Laboratories Co., Ltd.), p44/42, phospho-p44/42 (Thr^{202}/Tyr^{204}), phospho-Tie2 (Tyr^{992}) Abs (Cell Signaling Technology, Inc.) and mouse anti-HA (12CA5) mAb (Roche Diagnostics) were used as the first Abs. Anti-phospho-Tie2 (Tyr^{992}) and anti-phosphotyrosine Abs were diluted 1:500, and others were diluted 1:1000. HRP-conjugated anti-rabbit and anti-mouse IgG (Jackson ImmunoResearch Laboratories) was used as the secondary antibody (dilution: 1:1000). For the immunofluorescence analysis, HA and Myc were used as the first Abs (dilution, 1:100). Alexa Fluor 546-conjugated goat anti-rabbit Igs and Alexa Fluor 647-conjugated goat anti-mouse Igs were used as the secondary Abs (Invitrogen) (dilution, 1:200).

Plasmid Construction—Mouse Tie2 and Tie1 were fused to sequences encoding full-length Venus and Venus residues 1–173 amino acids (VN) or 155–238 amino acids (VC). The coding regions were connected with linker sequences encoding RSAIT (Arg-Ser-Ala-Ile-Thr). RSAIT is a non-adhesion sequence (26). HA or Myc epitopes were inserted as tags between linker and fluorescent genes. Genes were inserted at the multicloning site in pEGFPN1 vector or pMRX virus vector. Basing the work on the pE-Tie2-linker-Myc-Venus, pE-Tie2-linker-HA-VN and pE-Tie2-linker-Myc-VC, we cut between the BamHI and MluI sites and the Tie2 mutant (Tie2K854R, Tie2R848W) was created. Tie2 kinase-dead (Tie2K854R) or Tie2 constitutive-active (Tie2R848W) mutants were amplified from wild-type Tie2 using Tie2K854R-N, -C primers or Tie2R848W-N, -C primers, respectively (supplemental Table S1).

For the generation of Tie1*, the signal sequence of Tie2 was amplified from the Tie2 plasmid using oligonucleotide primers (forward primer, 5′-GTA GGC GTG TAC GGT GGG AGG TCT-3′ and reverse primer, 5′-GTT AAG TCA ACA GAG CCT TCT ACT ACT CC-3′) and 5′-Tie1 core sequence excluding signal sequence was amplified from Tie1 using oligonucleotide primers (forward primer, 5′-GGA GTA GTA GAA GGC TCT GTT GAC TTA AC-3′ and reverse primer, 5′-CCA CTT CTG AGC TTC ACA GCC TCG CAC GAT-3′). These two products were amplified with the forward primer for Tie2 and the reverse primer for Tie1. This PCR product was placed into EcoRI and AgeI sites of the Tie1 plasmid. For the generation of Tie2/Tie1 chimeric plasmids, mutagenesis was performed on Tie2 and Tie1 plasmids as templates by using specific primer sets (supplemental Table S1). For generation of 1–3 amino acid mutants of each Tie2 plasmid, mutagenesis was performed using specific primers (supplemental Table S1).

Retroviral Infection—Plat-E cells were transfected with pMRX-Tie2-linker-Myc-Venus, pMRX-Tie2YIA/LAS-linker-Myc-Venus, pMRX-Tie2-linker-HA-VN173 and pMRX-Tie2-linker-Myc-VC155, pMRX-Tie2YIA/LAS-linker-HA-VN173 and pMRX-Tie2YIA/LAS-linker-Myc-VC155 vectors as indicated in each experiment (1.0 μg each) using Lipofectamine 2000 (Invitrogen) and then incubated for 24 h at 37 °C after which the medium was changed. After 12 (36 h from transfection) and 24 h (48 h from transfection), conditioned medium was harvested, sterilized by filtration, and used to infect NIH3T3 cells. 8 μg/ml polybrene was added for enhancement of infection. Stable cell lines were selected by culture in medium containing puromycin (5 μg/ml) or blasticidin (10 μg/ml) (27, 28).

Cell Culture—HEK293T and NIH3T3 lines were grown in DMEM supplemented with 10% FBS. Platinum-E cells (Plat-E; packaging cells) and stable cell lines transfected by pMRX virus vector were cultured in 10% FBS containing DMEM.

Transfection and Bimolecular Fluorescence Complementation Analysis—To carry out BiFC in living cells, cells were co-transfected with the expression vectors indicated in each experiment (1.0 μg each) using Lipofectamine 2000. The fluorescence emissions were acquired in living cells 22–48 h after transfection using a fluorescence microscope with a cooled CCD camera, or by flow cytometry. Protein expression levels were assessed by Western blotting.

Cell Lysis, Immunoprecipitation, SDS-PAGE, and Western Blotting—Cells were washed with ice-cold PBS and lysed with radioimmune precipitation assay lysis buffer (50 mM Tris-HCl, pH 7.5, 150 mM NaCl, 1% Nonidet P-40, 0.5% sodium deoxycholate, 0.1% SDS). The cells were incubated on ice for 10 min followed by centrifugation at 15,000 rpm for 5 min at 4 °C. Cells were immunoprecipitated from the supernatant using 1–2 μg of anti-Myc Ab that had been precoupled to 20 μl of protein A-Sepharose 4 Fast Flow (GE Healthcare).

Proteins electrophoretically separated using 7.5% SDS gels were transferred to nylon membranes (Amersham Biosciences) by a wet blotting procedure (140 V, 200 mA, 120 min). The membrane was blocked with 5% skim milk/TBST for 60 min, subsequently incubated with the Abs as indicated in the figures and processed for chemiluminescence detection with ECL solution. Densitometry was performed with NIH ImageJ software (version 1.43u).

FACS Analysis—BiFC was analyzed by flow cytometry. After fluorescence complementation, cells were washed with PBS and resuspended in PBS. FACS analysis was performed with a FACSCalibur (BD Biosciences) using the 488 nm laser for excitation and a 515–545 nm band pass filter for detection. For quantitative evaluation of BiFC fluorescence, we used % Gated (fluorescent cells) × X Geo Mean (average of fluorescent intensity) as arbitrary fluorescence units.

Confocal Laser Scanning Microscopy—Transfected cells on 0.1% gelatin-coated glass dishes (Sigma Aldrich) were rinsed, fixed for 10 min in 4% paraformaldehyde-PBS (pH 7.5), and washed with PBS. Subsequently, the cells were permeabilized with 0.1% Triton X-100 for 10 min. After washing with PBS, cells were blocked with PBS containing 5% normal goat serum and 1% BSA for 30 min and immunostained with first Ab (1:100) for 1 h. Protein reacting with Ab was visualized with secondary Abs (1:200). HA or Myc epitopes were inserted as tags between Tie2 or Tie2YIA/LAS and the BiFC tag (VN or VC). HA-VN fused with Tie2 or Tie2YIA/LAS was stained by rabbit anti-HA Ab (Medical & Biological Laboratories Co., Ltd.) and Alexa Fluor 546 (red)-conjugated anti-rabbit Igs. Myc-VC fused with Tie2 or Tie2YIA/LAS was stained with

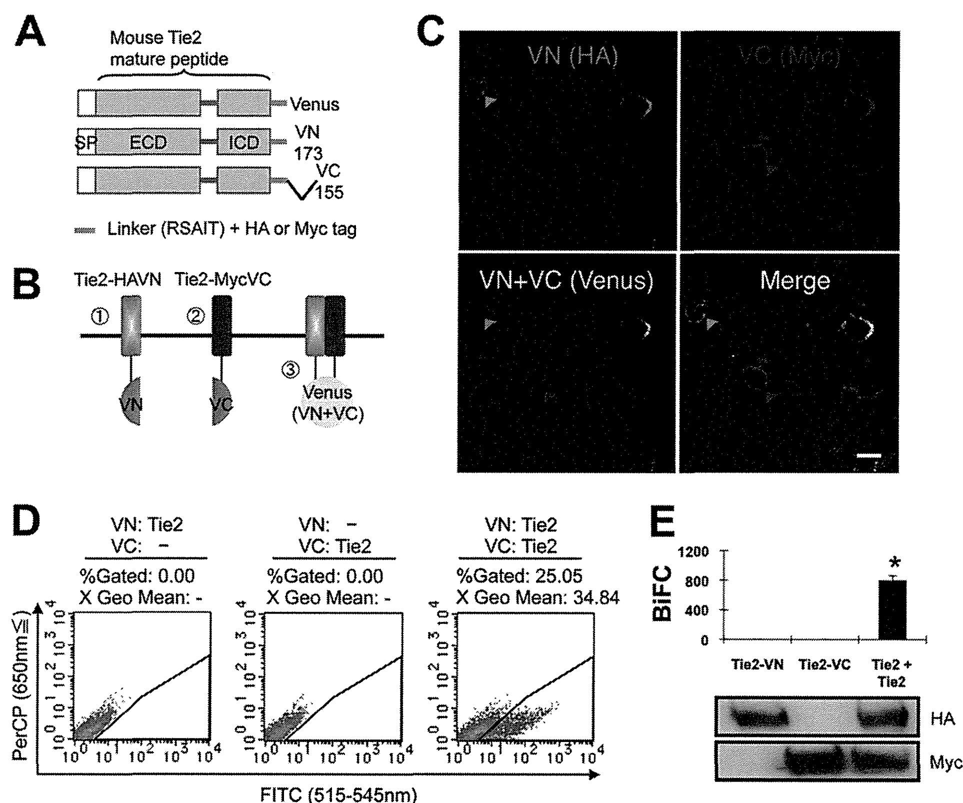

FIGURE 1. **BiFC analysis of Tie2 receptor homodimerization in living cells.** *A* and *B*, schematic representation of Tie2 tagged with either the N- or C-terminal of the Venus fragment (VN or VC). *SP*, signal peptide; *ECD*, extracellular domain; *ICD*, intracellular domain. When Tie2 dimerizes, fluorescence should reconstitute. *C*, HEK293T cells expressing Tie2-HAVN (*red*) and Tie2-MycVC (*blue*) observed by confocal microscopy. Cells were co-transefected with Tie2-HAVN and Tie2-MycVC expression vectors. Note that cells expressing Tie2-HAVN alone (*red arrowhead*) or Tie2-MycVC alone (*blue arrowhead*) develop no Venus fluorescence. *Bar* indicates 20 μm. *D*, flow cytometric analysis for evaluation of receptor dimerization as indicated. *E*, quantitative evaluation of Tie2 homodimerization in BiFC as observed in *D* (*, $p < 0.05$; $n = 3$). Protein expression level of each receptor was assessed by immunoblotting with anti-HA or anti-Myc Ab.

mouse anti-Myc Ab and Alexa Fluor 647 (blue)-conjugated anti-mouse Igs. BiFC fluorescence was detected using a filter for Alexa Fluor 488 (green). The slides were observed under a Leica TCS SP5 Ver1.6 (Leica Microsystems) using HCX PL APO lambda blue 63 × 1.4 oil. Images were processed using Adobe Photoshop CS5 Extended software (Adobe Systems).

Statistical Analysis—All data are displayed as the mean ± S.D. and were analyzed by two-tailed Student *t* test. A probability value of < 0.05 was considered statistically significant.

RESULTS

Establishment of Imaging Methods for Investigating the Dimerization of Tie2 Receptors—It has been reported that Tie2 is present in the form of dimers and/or oligomers on the cell surface (19). We also detected ligand-independent dimers of endogenous Tie2 in human umbilical vein endothelial cells (supplemental Fig. S1*A*). To assess Tie2 dimerization in the absence of Ang1, we utilized the BiFC assay (26). First, we prepared amino (N)-terminal (1–173: VN173) and carboxyl (C)-terminal (155–238: VC155) components of Venus fluorescent protein, a modifier of yellow fluorescent protein, fused with the C-terminal domain of wild-type (WT) mouse Tie2 with an HA or Myc tag linked to the molecule (Fig. 1*A*). When Tie2 (Tie2-HAVN, Tie2-MycVC) dimerizes, the fluorescent complex should be reconstituted (Fig. 1*B*). As expected, when Tie2-HAVN and Tie2-MycVC were cotransfected into HEK293T cells, cells expressing both HA and Myc developed fluorescence (Fig. 1*C*). Flow cytometry showed that transfection with both Tie2-HAVN and Tie2-MycVC vectors, but not with either alone, resulted in cells having high FITC intensity (Fig. 1, *D* and *E*). We confirmed that these co-transfectants developed BiFC fluorescence in cells expressing physiological levels of Tie2 as observed in ECs (supplemental Fig. S1, *B* and *C*).

Analysis of the Dimerization of Tie2-Tie1 using BiFC Assays—Ang1 activates Tie1 indirectly, mediated by its interaction with Tie2 (11, 12). It has been suggested that co-localization of Tie2 and Tie1 is induced upon activation of Tie2 by Ang1 (6). We investigated whether Tie2 and Tie1 also form heterodimers in a ligand-independent manner. Relative to Tie2, we found that the Tie1 protein was difficult to express in HEK293T cells following transfection of full-length Tie1 cDNA. However, when the original native signal sequence of Tie1 was excised and replaced with the Tie2 signal sequence (designated Tie1*), Tie1 expression was easily induced (Fig. 2*A*). Using this Tie1* construct, we evaluated Tie2-Tie1 and Tie1-Tie1 associations by BiFC. Although it has recently been reported that Tie2 and Tie1 associate following Ang1 stimulation and on cell-cell contact, we failed to detect any Tie2-Tie1 or Tie1-Tie1 associations (Fig. 2, *B–D*). This suggests that a Tie2 and Tie1 interaction is required for Ang1 binding to Tie2 and Tie1 and that Tie1 never gives rise to inactive dimers and/or oligomers in the absence of Ang1.

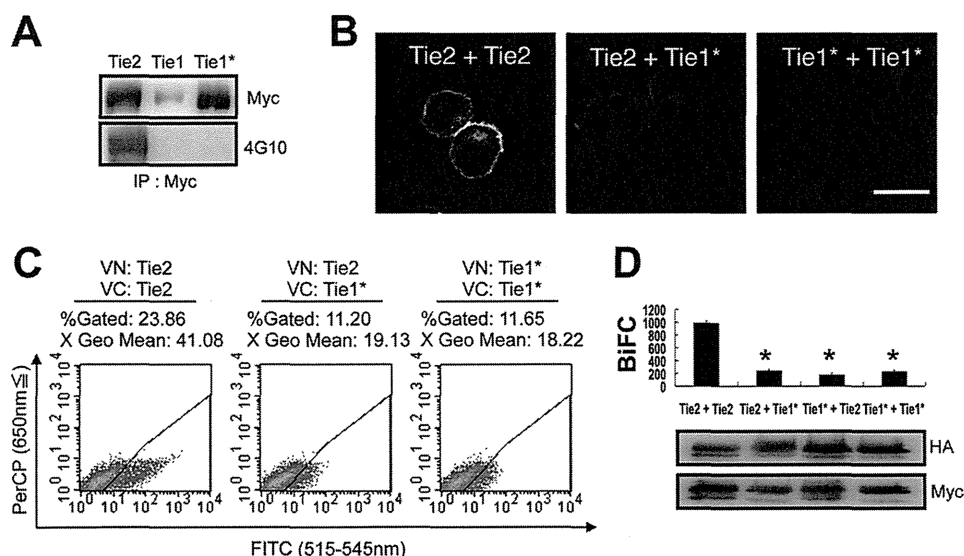

FIGURE 2. **BiFC analysis comparing Tie2 and Tie1*.** *A*, signal peptide of Tie1 was replaced with that of Tie2 (Tie1*). All receptors were C-terminally tagged with Myc. The levels of Tie2, Tie1, and Tie1* protein were analyzed with Myc or 4G10 Ab. *B–D*, HEK293T cells were transiently transfected in combination with Tie2-HAVN and Tie2-MycVC, Tie2-HAVN and Tie1*-MycVC, or Tie1*-HAVN and Tie1*-MycVC. *B*, cells were analyzed by confocal microscopy. *Bar* indicates 20 μm. *C*, flow cytometric analysis for evaluation of receptor dimerization as indicated. *D*, quantitative evaluation of receptor dimerization in BiFC as shown in *C* (*, $p < 0.05$; $n = 3$). Protein expression level of each receptor was assessed by immunoblotting with anti-HA or anti-Myc Ab.

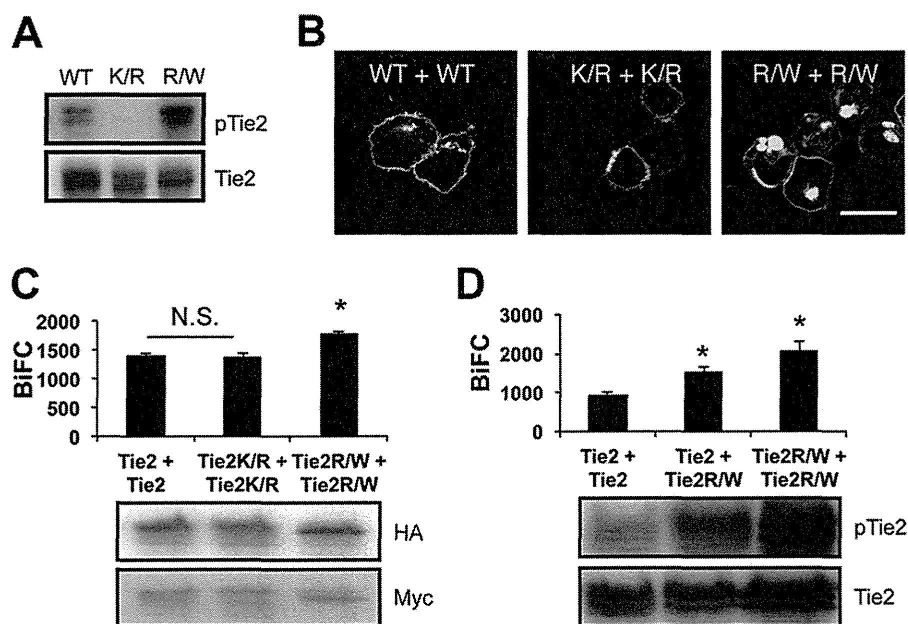

FIGURE 3. **BiFC analysis comparing Tie2 and Tie2 mutant.** *A*, detection of Tie2, kinase-dead mutant Tie2K854R (*K/R*) and constitutively active mutant Tie2R848W (*R/W*) phosphorylation. *B* and *C*, HEK293T cells were transiently transfected in combination with Tie2-HAVN and Tie2-MycVC, Tie2K854R-HAVN and Tie2K854R-MycVC, or Tie2R848W-HAVN and Tie2R848W-MycVC. *B*, cells were analyzed by confocal microscopy. *Bar* indicates 20 μm. *C*, quantitative evaluation of receptor dimerization in BiFC as shown in *B* (*, $p < 0.05$; $n = 3$). Protein expression level of each receptor was assessed by immunoblotting with anti-HA or anti-Myc Ab. *D*, quantitative evaluation of receptor dimerization in BiFC of Tie2 and Tie2R848W (*, $p < 0.05$; $n = 3$). Protein expression level of each receptor was assessed by immunoblotting with anti-Tie2. *N.S.*, not significant.

Analysis of the Dimerization of Tie2 Mutants Using BiFC Assays—Phosphorylation of overexpressed Tie1 and Tie2 was observed, but only Tie2 and not Tie1 was autophosphorylated in the absence of Ang1 stimulation (Fig. 2*A*). To test whether phosphorylation of Tie2 affects Tie2-Tie2 dimerization, we generated a kinase-inactive Tie2 mutant (Tie2K854R) (Fig. 3*A*). However, loss of phosphorylation did not affect Tie2 dimerization (Fig. 3, *B* and *C*, and supplemental Fig. S2A). We further confirmed that it was not until Ang1 bound Tie2 that dimerized Tie2 was internalized (supplemental Fig. S2*B*). Although dimerized WT Tie2 was observed in the cytoplasm, dimerized kinase-inactivated Tie2 did not internalize from the cell surface into the cytoplasm (Fig. 3*B*). Next, we constructed a constitutively active mutant of Tie2 (Tie2R848W) (Fig. 3*A*) (29). In HEK293T cells overexpressing Tie2R848W-HAVN and Tie2R848W-MycVC, more abundant Venus fluorescence was observed in the cytoplasm than in wt Tie2 or Tie2K854R (Fig. 3, *B* and *C*). Interestingly, Tie2R848W can dimerize with WT Tie2, resulting in BiFC intensity enhanced compared with Tie2-Tie2 dimers (Fig. 3*D*). These results suggest that our BiFC

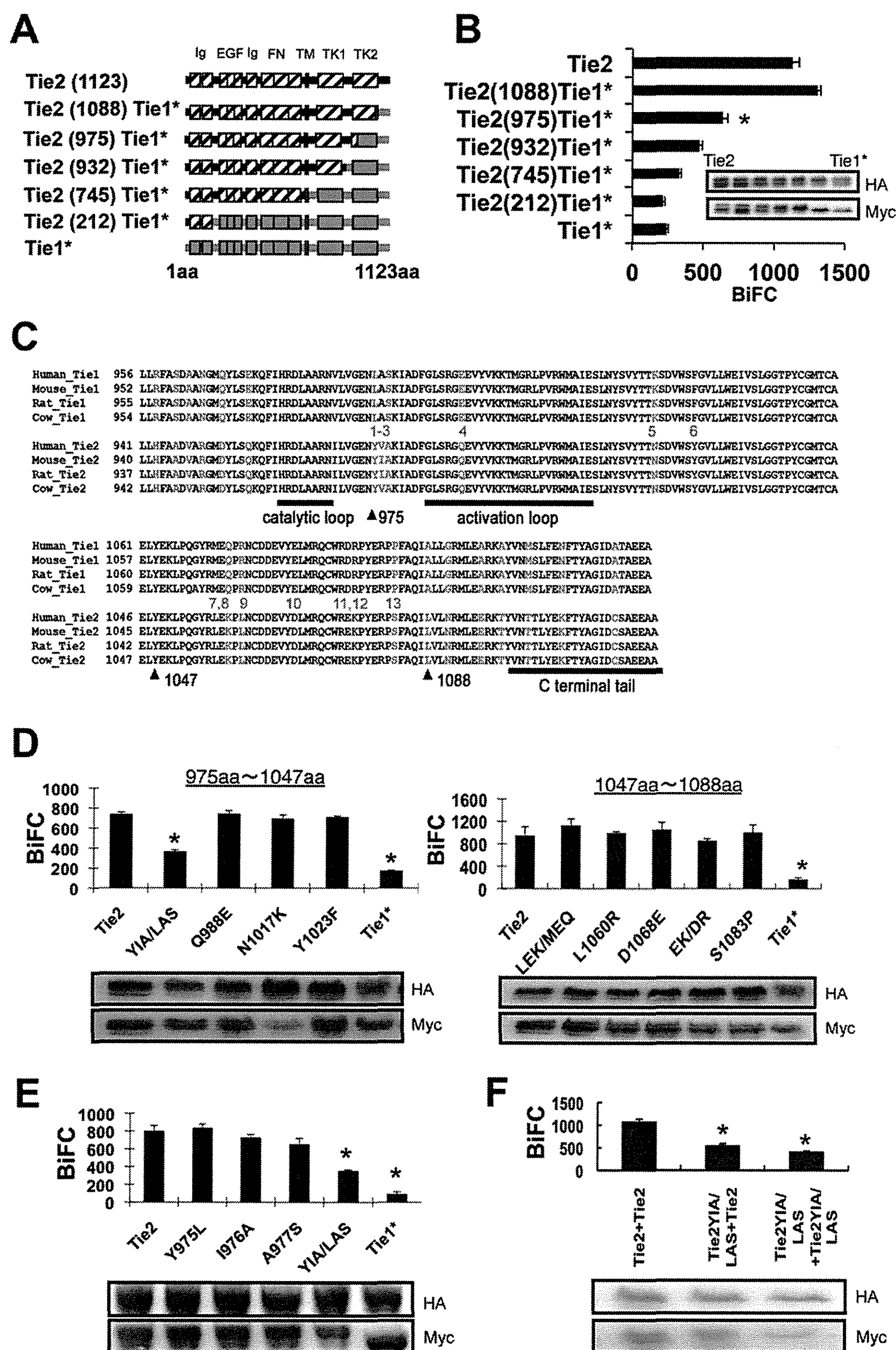

FIGURE 4. **YIA sequence of Tie2 induces ligand-independent dimerization.** *A*, schematic of Tie2/Tie1* chimeras. *B*, in HEK293T cells, Tie2-HAVN was transiently transfected in combination with Tie2, Tie2(1088)Tie1*, Tie2(975)Tie1*, Tie2(932)Tie1*, Tie2(745)Tie1*, Tie2(212)Tie1*, or Tie1* C-terminally fused with MycVC, and close associations of receptors assessed by BiFC and flow cytometry (*, $p < 0.05$; $n = 3$). The protein expression level of each receptor was confirmed by immunoblotting with anti-HA or anti-Myc Ab (*inset*). *C*, comparison of amino acid sequences of Tie1 and Tie2 C terminus from different species. *Pink*, different amino acids; *blue*, same amino acids (*aa*). *D* and *E*, in HEK293T cells, Tie2-HAVN was transiently transfected in combination with Tie2, Tie2YIA/LAS, Tie2Q988E, Tie2N1017K, Tie2Y1023F, Tie2LEK/MEQ, Tie2L1060R, Tie2D1068E, Tie2EK/DR, Tie2S1083P, or Tie1* C-terminally fused with MycVC (*D*) or Tie2, Tie2Y975L, Tie2I976A, Tie2A977S, Tie2YIA/LAS, or Tie1* C-terminally fused with MycVC (*E*), and close associations of receptors assessed by BiFC and flow cytometry. Protein expression level of each receptor was confirmed by immunoblotting with anti-HA or anti-Myc Ab (*inset*) (*, $p < 0.05$; $n = 3$). *F*, YIA domain of Tie2 was replaced by LAS sequence (Tie2YIA/LAS). Association of Tie2-Tie2, Tie2-Tie2YIA/LAS, and Tie2YIA/LAS-Tie2YIA/LAS was observed by BiFC as described above. Protein expression level of each receptor was confirmed by immunoblotting with anti-HA or anti-Myc Ab (*inset*) (*, $p < 0.05$; $n = 3$).

system mimics canonical receptor down-modulation only after activation of the receptor.

Identification of the Domain That Induces Ligand-independent Tie2 Homodimerization—We found that Tie2, but not Tie1, forms homodimers in a ligand-independent manner. Hence, we attempted to isolate the Tie2 ligand-independent dimerizing region. First, we sought domains responsible for Tie2-Tie2 association by replacing part of Tie2 with the Tie1 homologous domain (Fig. 4*A*). We found that lack of the extracellular domain of Tie2 did not affect BiFC (supplemental Fig. S3), suggesting that BiFC caused by Tie2-Tie2 interaction is mainly induced by the intracellular domain of Tie2 in our

model. Therefore, we focused on the intracellular domain of Tie2 for dimerization in our next experiments.

We transfected Tie2-HAVN and Tie2/Tie1* chimeric genes fused with Myc-tagged VC155 into HEK293T cells. When the C-terminal of Tie2 (from 975 to 1088 amino acids) was replaced by the Tie1 sequence, BiFC was significantly attenuated (Fig. 4*B*). There are differences in 13 amino acids between Tie2 and Tie1 (Fig. 4*C*). Therefore, we mutated Tie2 where its sequence is different from Tie1 domain by domain and observed Tie2-Tie2/mutant dimerization. We found that a YIA sequence within Tie2 (975–977) is critical for dimerization (Fig. 4*D*). Next, we introduced point mutations into this YIA domain. We found that no single mutation was responsible for reducing Tie2 dimerization, but rather the whole YIA tandem sequence was involved (Fig. 4*E*). We generated mutant Tie2 (Tie2YIA/LAS) in which the YIA domain of Tie2 was replaced by LAS. Tie2-Tie2YIA/LAS and Tie2YIA/LAS-Tie2YIA/LAS dimerization was not significantly different, suggesting that both Tie2 YIA domains in the cytoplasmic region are required for dimerization (Fig. 4*F*). When phosphorylation of Tie2YIA/LAS was assessed, it was found that mere overexpression did not induce it (supplemental Fig. S4).

Tie2YIA/LAS Monomer Mutants Can Be Dimerized and Phosphorylated by Ligand Binding—Tie2 can form ligand-independent inactive dimers; it has therefore been suggested that receptor dimerization and activation are mechanistically distinct and separable events (19, 30). Next, we analyzed whether Ang1 binding to the inactive monomer mutant Tie2YIA/LAS induced dimerization and activation of Tie2. Phosphorylation of WT Tie2 by exogenous Ang1 did not increase the intensity of BiFC developed by either Tie2-Tie2 (Fig. 5*A*). On the contrary, Ang1 stimulation decreased BiFC intensity after 30 min. This suggests that internalization and degradation of Tie2 was induced after Tie2 phosphorylation (30). Interestingly, we found that Tie2YIA/LAS prominently enhanced BiFC intensity under Ang1 stimulation for 1 h (Fig. 5*B*). Microscopy showed that Tie2 formed ligand-independent dimers and was internalized upon Ang1 stimulation (Fig. 6*A*). In contrast, Tie2YIA/LAS dimerization was not detected in the absence of Ang1. However, BiFC signals due to dimerization did occur upon stimulation with Ang1, although to a lesser extent than in WT Tie2. This suggests that YIA mutations in Tie2 did not completely prevent Tie2 dimerization (Fig. 6*B*).

Finally, we investigated how the lack of Tie2 ligand-independent dimerization affected its phosphorylation and downstream Erk signaling. When the time course of Tie2 phosphorylation was recorded in the presence of a fixed dose of Ang1 (200 ng/ml), no significant differences between wild-type Tie2 and Tie2YIA/LAS were observed (Fig. 7*A*). However, when phosphorylation was measured after stimulation for 10 min with different doses of Ang1, Tie2 and Erk phosphorylation by Tie2YIA/LAS decreased at a high dose (350~500 ng/ml) of Ang1 compared with wild-type Tie2 (Fig. 7, *B* and *C*). These findings suggest that the YIA domain of Tie2 is not indispensable for dimerization of Tie2 but is used for forming non-ligand-mediated dimerization of Tie2 to effectively react to a higher dose of Ang1.

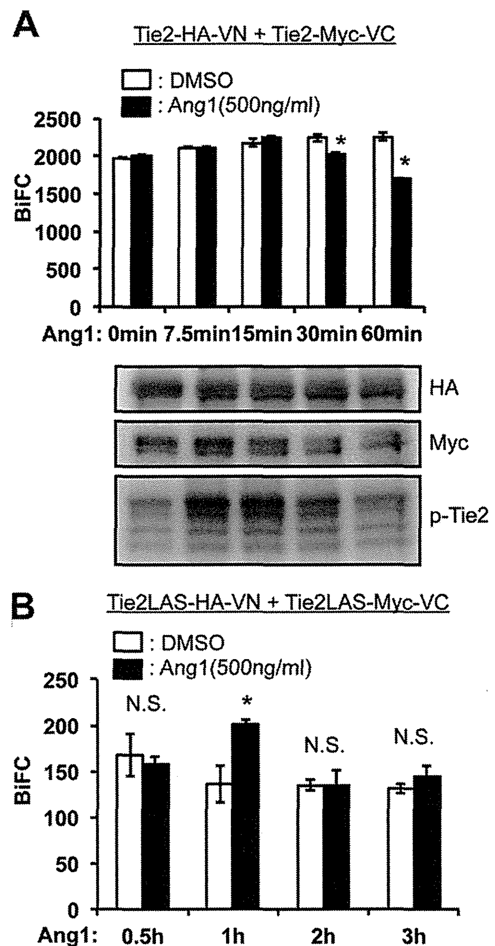

FIGURE 5. **BiFC analysis of ligand-dependent dimerization of Tie2.** *A*, dimerization of Tie2 was observed in Tie2-VN- and Tie2-VC-coexpressing NIH3T3 cells in the presence or absence of Ang1 stimulation. At each time point, cell lysates were analyzed for Tie2-HAVN and Tie2-MycVC as well as the degree of Tie2 phosphorylation (*lower panel*). Note that Ang1 stimulation did not enhance BiFC level but rather attenuated it 30 min after stimulation with Ang1. *B*, time course of dimerization of Tie2YIA/LAS (Tie2LAS) was observed in Tie2 YIA/LAS-VN- and Tie2 YIA/LAS -VC-coexpressing HEK293T cells in the presence or absence of Ang1 stimulation (*, $p < 0.05$; $n = 3$). *DMSO*, dimethyl sulfoxide; *N.S.*, not significant.

DISCUSSION

In the present study, we visualized Tie2 dimerization by the BiFC method and sought ligand-independent dimerization domains of Tie2. A previous report showed that Tie2 clusters are expressed on the apical and basolateral plasma membranes (19). However, it was not clear whether Tie2 phosphorylation results in dimer formation. Here, we showed that kinase-inactive Tie2 mutants also form dimers in the absence of Ang1. Thus, Tie2 can indeed form dimers without Ang1. To analyze the role of ligand-independent dimerization of Tie2, a mutant that cannot form dimers in the absence of Ang1 is required. In the present study, we utilized a mutant with no evidence of Tie1-Tie1 dimerization even when overexpressed. Based on the amino acid sequence difference between Tie2 and Tie1, we found that YIA in the Tie2 cytoplasmic domain is important for ligand-independent Tie2 dimerization.

We show that the YIA domain required to form ligand-independent Tie2 dimers is situated between the catalytic and activation loops in the intracellular region of the molecule. Previ-

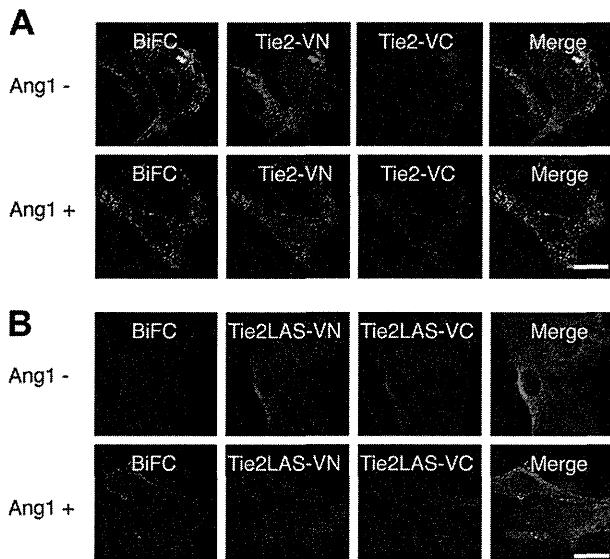

FIGURE 6. **Tie2YIA/LAS cannot form ligand-independent dimers but is dimerized and phosphorylated upon stimulation with Ang1.** *A*, dimerization and localization of Tie2 were observed in Tie2-VN- and Tie2-VC-coexpressing NIH3T3 cells in the presence or absence of Ang1. Wild-type Tie2 can form dimers irrespective of Ang1 stimulation, as confirmed by BiFC. However, this dimerized Tie2 forms cluster-like aggregations and is internalized upon stimulation with Ang1. *B*, similar to *A*, dimerization and localization of Tie2YIA/LAS (Tie2LAS) is observed in Tie2YIA/LAS-VN- and Tie2YIA/LAS-VC-coexpressing NIH3T3 cells. In the absence of Ang1, Tie2LAS did not dimerize but formed cluster-like aggregations upon stimulation with Ang1. *Bar* indicates 20 μm.

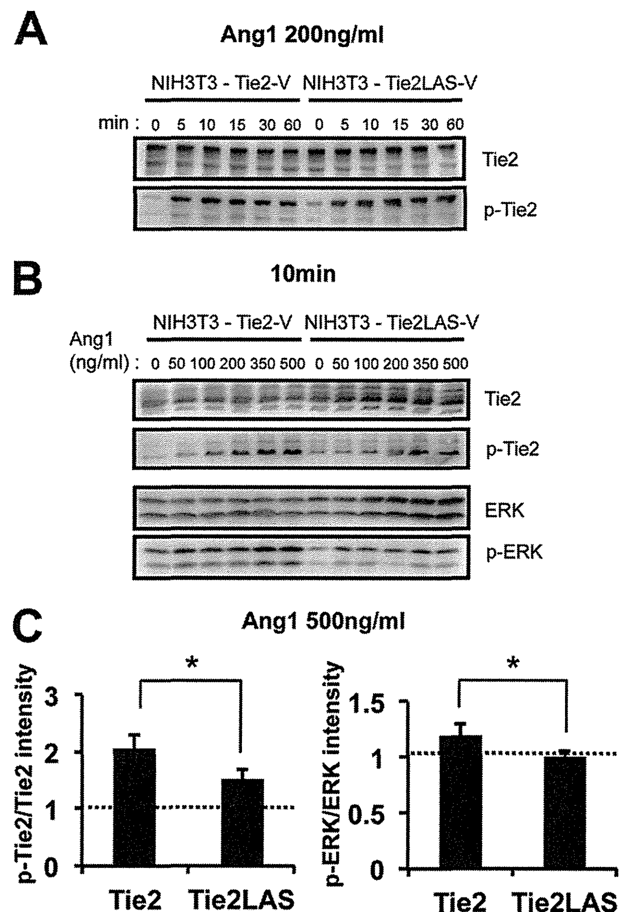

FIGURE 7. **Phosphorylation of Tie2 and Tie2 downstream molecule Erk.** *A*, Ang1 reactivity of Tie2 and Tie2YIA/LAS. After exposure to 200 ng/ml of Ang1, Tie2 and Tie2YIA/LAS phosphorylation was detected in a time-dependent fashion between 0 and 60 min. *B*, Ang1 reactivity of Tie2 and Tie2YIA/LAS. Ang1-mediated Tie2, Tie2YIA/LAS, and Erk phosphorylation was detected in a dose-dependent fashion between 0 and 500 ng/ml for 10 min. *C*, Tie2 and Erk phosphorylation on stimulation with 500 ng/ml Ang1 was quantified. The ratio of pTie2/Tie2 or pErk/Erk in cells on stimulation with Ang1 was compared with Ang1-untreated cells. (*, $p < 0.05$; $n = 3$).

ous reports show that the Tie2 C-terminal tail has a negative regulatory role in Tie2 signaling and function (31, 32). To activate Tie2, conformational changes in the intracellular loop structure and C-terminal tail are required for ATP and substrate binding. Therefore, it is possible that YIA domains control the movement of these loop and C-terminal tails. Further structural analysis of Tie2 will be necessary to assess how the YIA domain controls ligand-independent dimerization of Tie2 for folding and Tie2-Tie2 associations.

Unlike Tie2 homodimer formation, the BiFC method reveals that Tie2 and Tie1 scarcely interact. Recently, it has been reported that Tie2-Tie1 heterodimer formation is induced in the extracellular domain of Tie2 and Tie1, respectively, and that this occurs in the absence of angiopoietin ligation (33). Heterodimerization was observed using Tie receptors lacking intracellular domains. At present, it is difficult to explain this discrepancy, but it may simply be due to the absence of receptor cytoplasmic regions in the previous report. Indeed, when endogenous Tie2 and Tie1 localization in human umbilical vein endothelial cells was observed in the absence of Ang1, we found that Tie2 and Tie1 did not co-localize on the cell surface (supplemental Fig. S5). However, as previously reported, upon Ang1 stimulation, co-localization of these receptors does occur. In contrast, when NIH3T3 cells expressing Tie2-VN and Tie1*-VC were stimulated with Ang1, BiFC intensity was not enhanced (supplemental Fig. S6*A*). In addition, Ang1 activates both Tie2 and Tie1, but we did not observe a strong physical association between Tie2 and Tie1 in the immunoprecipitation analysis (supplemental Fig. S6, *B* and *C*). It has been reported that shedding of Tie1 extracellular domain itself induces Tie2 activation and that Ang2 acts as a Tie2 agonist upon Tie1 shedding (34–36). This suggests that Tie1 ectodomain shedding plays important roles in promoting Tie2 conformation changes and activation. Therefore, we cannot completely exclude the possibility that full-length Tie2 and Tie1 may heterodimerize under certain specific conditions in ECs.

It has been reported that Tie2 forms oligomers on the cell membrane (19); however, the function of such forms of Tie2 has not been elucidated. We found that a lack of ligand-independent dimerization of Tie2 led to attenuation of high dose Ang1-mediated activation of Tie2. This suggests that ligand-independent Tie2 dimerization plays a role in the rapid clustering of Tie2 upon activation with higher doses of Ang1 or in the preformation of Tie2 oligomers to respond to higher doses of Ang1. Further precise analysis of how ligand-independent dimerization of Tie2 relates to the extent of Tie2 phosphorylation at higher Ang1 doses is still required, including elucidation of the biological significance of Tie2 oligomers.

In humans, an amino acid substitution of tryptophan for arginine at residue (Tie2R849W) leads to ligand-independent constitutive activation; it is associated with familial venous malformations and causes thickness or lack of smooth muscle cells

in the veins systemically (14, 29, 37). In the present study, we showed that the intensity of BiFC signals from Tie2R848W-Tie2R848W was enhanced. Interestingly, Tie2R848W interactions with WT Tie2 were stronger than Tie2-Tie2 interactions. This suggests that Tie2R848W may heterodimerize with WT Tie2 and induce constitutive phosphorylation of WT Tie2. Therefore, analysis of regulatory mechanisms in ligand-independent dimerization domains may be useful for developing therapeutic strategies to inhibit Tie2 activation in patients suffering from venous malformation.

Acknowledgments—We thank T. Kamimoto, N. Fujimoto, and K. Fukuhara for technical assistance.

REFERENCES

1. Dejana, E., Tournier-Lasserve E., and Weinstein, B. M. (2009) The control of vascular integrity by endothelial cell junctions: molecular basis and pathological implications. *Dev. Cell* **16,** 209–221
2. Augustin, H. G., Koh, G. Y., Thurston, G., and Alitalo, K. (2009) Control of vascular morphogenesis and homeostasis through the angiopoietin-Tie system. *Nat. Rev. Mol. Cell Biol.* **10,** 165–177
3. Sato, T. N., Tozawa, Y., Deutsch, U., Wolburg-Buchholz, K., Fujiwara, Y., Gendron-Maguire, M., Gridley, T., Wolburg, H., Risau, W., and Qin, Y. (1995) Distinct roles of the receptor tyrosine kinases Tie-1 and Tie-2 in blood vessel formation. *Nature* **376,** 70–74
4. Davis, S., Aldrich, T. H., Jones, P. F., Acheson, A., Compton, D. L., Jain, V., Ryan, T. E., Bruno, J., Radziejewski, C., Maisonpierre, P. C., and Yancopoulos, G. D. (1996) Isolation of angiopoietin-1, a ligand for the TIE2 receptor, by secretion-trap expression cloning. *Cell* **87,** 1161–1169
5. Fukuhara, S., Sako, K., Minami, T., Noda, K., Kim, H. Z., Kodama, T., Shibuya, M., Takakura, N., Koh, G. Y., and Mochizuki, N. (2008) Differential function of Tie2 at cell-cell contacts and cell-substratum contacts regulated by angiopoietin-1. *Nat. Cell Biol.* **10,** 513–526
6. Saharinen, P., Eklund, L., Miettinen, J., Wirkkala, R., Anisimov, A., Winderlich, M., Nottebaum, A., Vestweber, D., Deutsch, U., Koh, G. Y., Olsen, B. R., and Alitalo, K. (2008) Angiopoietins assemble distinct Tie2 signalling complexes in endothelial cell-cell and cell-matrix contacts. *Nat. Cell Biol.* **10,** 527–537
7. Takakura, N., Watanabe, T., Suenobu, S., Yamada, Y., Noda, T., Ito, Y., Satake, M., and Suda, T. (2000) A role for hematopoietic stem cells in promoting angiogenesis. *Cell* **102,** 199–209
8. Dumont, D. J., Gradwohl, G., Fong, G. H., Puri, M. C., Gertsenstein, M., Auerbach, A., and Breitman, M. L. (1994) Dominant-negative and targeted null mutations in the endothelial receptor tyrosine kinase, tek, reveal a critical role in vasculogenesis of the embryo. *Genes Dev.* **8,** 1897–1909
9. Puri, M. C., Rossant, J., Alitalo, K., Bernstein, A., and Partanen, J. (1995) The receptor tyrosine kinase TIE is required for integrity and survival of vascular endothelial cells. *EMBO J.* **14,** 5884–5891
10. Puri, M. C., Partanen, J., Rossant, J., and Bernstein, A. (1999) Interaction of the TEK and TIE receptor tyrosine kinases during cardiovascular development. *Development* **126,** 4569–4580
11. Saharinen, P., Kerkelä, K., Ekman, N., Marron, M., Brindle, N., Lee, G. M., Augustin, H., Koh, G. Y., and Alitalo, K. (2005) Multiple angiopoietin recombinant proteins activate the Tie1 receptor tyrosine kinase and promote its interaction with Tie2. *J. Cell Biol.* **169,** 239–243
12. Yuan, H. T., Venkatesha, S., Chan, B., Deutsch, U., Mammoto, T., Sukhatme, V. P., Woolf, A. S., and Karumanchi, S. A. (2007) Activation of the orphan endothelial receptor Tie1 modifies Tie2-mediated intracellular signaling and cell survival. *FASEB J.* **21,** 3171–3183
13. Patan, S. (1998) TIE1 and TIE2 receptor tyrosine kinases inversely regulate embryonic angiogenesis by the mechanism of intussusceptive microvascular growth. *Microvasc. Res.* **56,** 1–21
14. Morris, P. N., Dunmore, B. J., Tadros, A., Marchuk, D. A., Darland, D. C., D'Amore, P. A., and Brindle, N. P. (2005) Functional analysis of a mutant form of the receptor tyrosine kinase Tie2 causing venous malformations. *J. Mol. Med.* **83,** 58–63
15. Maisonpierre, P. C., Suri, C., Jones, P. F., Bartunkova, S., Wiegand, S. J., Radziejewski, C., Compton, D., McClain, J., Aldrich, T. H., Papadopoulos, N., Daly, T. J., Davis, S., Sato, T. N., and Yancopoulos, G. D. (1997) Angiopoietin-2, a natural antagonist for Tie2 that disrupts *in vivo* angiogenesis. *Science* **277,** 55–60
16. Thomas, M., and Augustin, H. G. (2009) The role of the Angiopoietins in vascular morphogenesis. *Angiogenesis* **12,** 125–137
17. Eklund, L., and Olsen, B. R. (2006) Tie receptors and their angiopoietin ligands are context-dependent regulators of vascular remodeling. *Exp. Cell Res.* **312,** 630–641
18. Kim, I., Kim, J. H., Moon, S. O., Kwak, H. J., Kim, N. G., Koh, G. Y. (2000) Angiopoietin-2 at high concentration can enhance endothelial cell survival through the phosphatidylinositol 3'-kinase/Akt signal transduction pathway. *Oncogene* **19,** 4549–4552
19. Bogdanovic E., Coombs N., and Dumont D. J. (2009) Oligomerized Tie2 localizes to clathrin-coated pits in response to angiopoietin-1. *Histochem. Cell Biol.* **132,** 225–237
20. Jura, N., Endres, N. F., Engel, K., Deindl, S., Das, R., Lamers, M. H., Wemmer, D. E., Zhang, X., and Kuriyan, J. (2009) Mechanism for activation of the EGF receptor catalytic domain by the juxtamembrane segment. *Cell* **137,** 1293–1307
21. Red Brewer, M., Choi, S. H., Alvarado, D., Moravcevic, K., Pozzi, A., Lemmon, M. A., and Carpenter, G. (2009) The juxtamembrane region of the EGF receptor functions as an activation domain. *Mol. Cell* **34,** 641–651
22. Yu, X., Sharma, K. D., Takahashi, T., Iwamoto, R., and Mekada, E. (2002) Ligand-independent dimer formation of epidermal growth factor receptor (EGFR) is a step separable from ligand-induced EGFR signaling. *Mol. Biol. Cell* **13,** 2547–2557
23. Tao, R. H., and Maruyama, I. N. (2008) All EGF (ErbB) receptors have preformed homo- and heterodimeric structures in living cells. *J. Cell Sci.* **121,** 3207–3217
24. Livnah, O., Stura, E. A., Middleton, S. A., Johnson, D. L., Jolliffe, L. K., and Wilson, I. A. (1999) Crystallographic evidence for preformed dimers of erythropoietin receptor before ligand activation. *Science* **283,** 987–990
25. Chan, F. K., Chun, H. J., Zheng, L., Siegel, R. M., Bui, K. L., and Lenardo, M. J. (2000) A domain in TNF receptors that mediates ligand-independent receptor assembly and signaling. *Science* **288,** 2351–2354
26. Kerppola, T. K. (2006) Design and implementation of bimolecular fluorescence complementation (BiFC) assays for the visualization of protein interactions in living cells. *Nat. Protocols* **1,** 1278–1286
27. Morita, S., Kojima, T., and Kitamura, T. (2000) Plat-E: an efficient and stable system for transient packaging of retroviruses. *Gene Ther.* **7,** 1063–1066
28. Saitoh, T., Nakano, H., Yamamoto, N., and Yamaoka, S. (2002) Lymphotoxin-β receptor mediates NEMO-independent NF-κB activation. *FEBS Lett.* **532,** 45–51
29. Vikkula, M., Boon, L. M., Carraway, K. L., 3rd, Calvert, J. T., Diamonti, A. J., Goumnerov, B., Pasyk, K. A., Marchuk, D. A., Warman, M. L., Cantley, L. C., Mulliken, J. B., and Olsen, B. R. (1996) Vascular dysmorphogenesis caused by an activating mutation in the receptor tyrosine kinase TIE2. *Cell* **87,** 1181–1190
30. Bogdanovic, E., Nguyen, V. P., and Dumont, D. J. (2006) Activation of Tie2 by angiopoietin-1 and angiopoietin-2 results in their release and receptor internalization. *J. Cell Sci.* **119,** 3551–3560
31. Shewchuk, L. M., Hassell, A. M., Ellis, B., Holmes, W. D., Davis, R., Horne, E. L., Kadwell, S. H., McKee, D. D., and Moore, J. T. (2000) Structure of the Tie2 RTK domain: self-inhibition by the nucleotide binding loop, activation loop, and C-terminal tail. *Structure* **8,** 1105–1113
32. Niu, X. L., Peters, K. G., and Kontos, C. D. (2002) Deletion of the carboxyl terminus of Tie2 enhances kinase activity, signaling, and function. Evidence for an autoinhibitory mechanism. *J. Biol. Chem.* **277,** 31768–31773
33. Seegar, T. C., Eller, B., Tzvetkova-Robev, D., Kolev, M. V., Henderson, S. C., Nikolov, D. B., and Barton, W. A. (2010) Tie1-Tie2 interactions mediate functional differences between angiopoietin ligands. *Mol. Cell* **37,** 643–655
34. Yabkowitz, R., Meyer, S., Black, T., Elliott, G., Merewether, L. A., and Yamane, H. K. (1999) Inflammatory cytokines and vascular endothelial

growth factor stimulate the release of soluble tie receptor from human endothelial cells via metalloprotease activation. *Blood* **93,** 1969–1979

35. Marron, M. B., Singh, H., Tahir, T. A., Kavumkal, J., Kim, H. Z., Koh, G. Y., and Brindle, N. P. (2007) Regulated proteolytic processing of Tie1 modulates ligand responsiveness of the receptor-tyrosine kinase Tie2. *J. Biol. Chem.* **282,** 30509–30517
36. Singh, H., Milner, C. S., Aguilar Hernandez, M. M., Patel, N., and Brindle, N. P. (2009) Vascular endothelial growth factor activates the Tie family of receptor tyrosine kinases. *Cell Signal.* **21,** 1346–1350
37. Limaye, N., Wouters, V., Uebelhoer, M., Tuominen, M., Wirkkala, R., Mulliken, J. B., Eklund, L., Boon, L. M., and Vikkula, M. (2009) Somatic mutations in angiopoietin receptor gene TEK cause solitary and multiple sporadic venous malformations. *Nat. Genet.* **41,** 118–124

The American Journal of Pathology, Vol. 182, No. 5, May 2013

ELSEVIER

The American Journal of
PATHOLOGY

ajp.amjpathol.org

TUMORIGENESIS AND NEOPLASTIC PROGRESSION

Possible Role of Mural Cell—Covered Mature Blood Vessels in Inducing Drug Resistance in Cancer-Initiating Cells

Takahiro Matsui,*† Yumi Kinugasa,* Hidekazu Tahara,*‡ Yuzuru Kanakura,† and Nobuyuki Takakura*§

From the Department of Signal Transduction, Research Institute for Microbial Diseases, and the Department of Hematology and Oncology,† Osaka University Graduate School of Medicine, Osaka University, Osaka; the Department of Urology,‡ Kyoto Prefectural University of Medicine, Kyoto; and Japan Science and Technology Agency (JST),§ K's Gobancho, Tokyo, Japan*

Accepted for publication January 7, 2013.

Address correspondence to Nobuyuki Takakura, M.D., Ph.D., Department of Signal Transduction, Research Institute for Microbial Diseases, Osaka University, 3-1 Yamada-oka, Suita, Osaka 565-0871, Japan. E-mail: ntakaku@biken.osaka-u.ac.jp.

Cancer recurrence has been suggested to be induced by residual cancer-initiating cells (CICs) or cancer stem cells (CSCs) after chemotherapy. Moreover, it is possible that CICs/CSCs acquire more aggressive behavior after therapy as shown by invasion and metastasis. In the cancer microenvironment, CICs/CSCs may localize in a specific area, the so-called stem cell niche, and isolation of this niche is important to elucidate the molecular mechanism of how CICs/CSCs acquire malignancy. We analyzed whether CICs acquire drug resistance after cancer drug treatment in a tumor cell allograft model in which we could identify and isolate living CICs by detecting a higher level of transcriptional activity of the *PSF1* gene promoter. In our models using Lewis lung carcinoma (LLC) mouse lung cancer and colon26 mouse colon cancer cell lines, we found that CICs in both tumors acquired drug resistance after cancer drug treatment. Interestingly, response to the anticancer drug was quite different between LLC and colon26 original tumors (ie, the proportion of CICs in LLC tumors increased but in colon26 tumors the proportion decreased). We found that CICs frequently localized near mature blood vessels in which endothelial cells were covered with mural cells and that the incidence of mature blood vessels in LLC tumors was four times higher than in colon26 tumors. These results suggest a relationship between mature blood vessels and CIC drug resistance. *(Am J Pathol 2013, 182: 1790—1799; http://dx.doi.org/10.1016/j.ajpath.2013.01.019)*

A recent concept has suggested that the recurrence of cancer is induced by cancer-initiating cells (CICs)/cancer stem cells (CSCs) that are resistant to conventional chemoradiotherapy.[1,2] They are defined as malignant cancer cells. Moreover, cells in this population have a greater ability to spread to other organs to form metastatic lesions and to digest matrices for invasion even during chemotherapy. In addition, a poor prognosis in a diverse set of human and mouse malignancies was associated with the expression of an embryonic stem cell—like genetic program,[3–5] suggesting that CSCs express an embryonic stem cell—specific genetic code. There is no doubt that CSC death is crucial for a permanent cancer cure.

It is widely accepted that CSCs/CICs have multidrug resistance and radiotherapy resistance mediated by activation of DNA damage responses.[6] In addition, the association of CSCs/CICs with the expression of multidrug-resistant genes was reported.[7] For example, ABCB5 is well known to play a role in drug resistance, and is one of a number of molecules proposed as a marker of CSC melanoma.[7,8] In a human breast cancer cell line, ABCB1 is co-regulated with CD44 expression (one of the CSC markers).[9] Moreover, it was reported that CD133, which is used as a stem cell marker, promotes up-regulation of ABCB1 and higher ABC transporter activity in rat glioma cells.[10] Another possibility is that cancer stromal cells in the tumor microenvironment prevent CSC cell death by several cues through the interaction between CSCs and stromal cells. In organs and tissues, the stem cell population localizes in a specific area, the so-called niche, and the interaction between stem cells and cells composing the niche is important to maintain the stemness of stem cells, such as self-renewal, immature status, and dormancy in such a niche.[11]

In the field of hematopoiesis, the niche has been analyzed extensively. The vascular niche was suggested to be important

Supported by a Grant-in-Aid for Scientific Research from the Ministry of Education, Culture, Sports, Science and Technology and the Japan Society for the Promotion of Science of Japan.

Copyright © 2013 American Society for Investigative Pathology.
Published by Elsevier Inc. All rights reserved.
http://dx.doi.org/10.1016/j.ajpath.2013.01.019

for self-renewal of hematopoietic stem cells (HSCs) because proliferation of HSCs was observed in vascular areas in embryos and in adult bone marrow.[12,13] On the other hand, HSC quiescence is induced in the osteoblastic niche where osteoblasts adhere to endosteum in the bone marrow.[14] Several tumor models have proposed that CSCs also may localize in vascular areas.[15,16] In a skin cancer model, vascular endothelial growth factor derived from CSCs expanded the vascular area, including the number of blood vessels, and resulted in the proliferation of CSCs.[17] On the other hand, although not connected with the localization of CSCs, it has been suggested that hepatocyte growth factor derived from myofibroblasts maintains the stemness of CSCs in colon cancer indirectly via the frizzled/Wnt pathway and that myofibroblast-secreted factors play pivotal roles in the induction of cancer cells into malignant CSCs.[18] Myofibroblasts are α-smooth muscle actin (α-SMA)–positive cells that usually localize near blood vessels and may work as a mural cell population. Therefore, based on previous reports, the vascular niche in which endothelial cells are covered with α-SMA–positive cells may maintain the stemness of CSCs; however, this has not been verified yet. Therefore, it is important to evaluate whether mural cell–covered blood vessels work as a niche for CSC/CICs.

For the evaluation of drug resistance, CSCs or CICs should be isolated as living cells from the tumor that has remained after therapy and it should be observed whether those cell types indeed do form secondary tumors. Several methods have been suggested for the detection of CSCs/CICs (ie, surface expression of CD133, surface-high expression of CD44 and negative-low expression of CD24, and high aldehyde dehydrogenase activity). However, data obtained by these methods have not always resulted in the same conclusion in mice. Therefore, we have generated a new technique to identify CICs by using promoter activity of the partner of sld five 1 (*Psf1*) gene (PSF1-promoter), a member of the GINS complex (from the Japanese go-ichi-ni-san meaning 5-1-2-3, derived from four related subunits of the complex Sld5, Psf1, Psf2 and Psf3), which is required for DNA replication by associating with CDC45 in yeast.[19] PSF1 protein is composed of coiled-coil, arginine-rich, and PEST-like domains from the N to the C terminus, and the C-terminal domain of PSF1 is crucial for chromatin binding and replication activity.[20] PSF1 expression was observed abundantly in bone marrow, thymus, and testis in mice.[21] Immature cell populations and stem cell populations express PSF1 [ie, epiblasts during embryogenesis, bone marrow hematopoietic stem cell populations, sperm stem cells (spermatogonia), and others] in mice.[21–23] Based on the phenotypes of mutant mice, PSF1 expression was required for acute proliferation of immature cell types such as epiblasts in embryos[21] and HSCs after bone marrow ablation.[23] The PSF1 in mice comprises the GINS complex, as observed in yeast. Therefore, it is possible that PSF1 is involved in the formation of DNA replication in mammals; however, the function of PSF1 has not been clarified in mice yet.

We found that promoter activity of the *Psf1* gene correlated with cancer cell malignancy.[16] When cells containing high or low levels of PSF1-promoter activity were compared, PSF1-promoter^{high} cancer cells had high proliferative activity, serial transplantation potential, and metastatic ability. Moreover, PSF1-promoter^{high} cancer cells displayed embryonic stem cell–like gene expression signatures. These results suggest that PSF1-promoter^{high} cancer cells are CICs. In the present work, we analyzed the *in vitro* and *in vivo* drug resistance of PSF1-promoter^{high} cancer cells and analyzed the microenvironment that supports the drug resistance of PSF1-promoter^{high} cancer cells.

Materials and Methods

Cell Culture

Lewis lung carcinoma (LLC) cells or colon26 (mouse colon cancer) cells were maintained in Dulbecco's modified Eagle's medium (Sigma-Aldrich, St. Louis, MO) or RPMI 1640 (Sigma-Aldrich), respectively, with 10% fetal bovine serum (Equitech-Bio, Kerville, TX) and penicillin/streptomycin. Colon26 cells or LLC cells expressing enhanced green fluorescent protein (EGFP) under the transcriptional control of the PSF1-promoter (colon26-*PSF1p-EGFP* or LLC-*PSF1p-EGFP*) were generated as previously reported.[16]

Mice

Seven- to 8-week-old C57BL/6 female mice (for LLC experiments), BALB/c female mice of the same age (for colon26 experiments), and 6- to 7-week-old KSN female nude mice were purchased from Japan SLC (Shizuoka, Japan). All animal studies were approved by the Osaka University Animal Care and Use Committee. Subcutaneous allografts were established by injecting 10^6 cells into the backs of mice. Tumor volume was measured with a caliper and calculated according to the following formula: $V = \text{width} \times \text{width} \times \text{length} \times 0.5$.

Anticancer Agent Administration

On day 7 after subcutaneous inoculation of cancer cells as described earlier, mice were treated with intraperitoneal injections of saline, 60 mg/kg body weight 5-fluorouracil (5-FU; Kyowa Hakko Kirin, Tokyo, Japan), or 5 mg/kg body weight cisplatin (Bristol-Myers, Tokyo, Japan) every other day. LLC-*PSF1p-EGFP*–bearing mice were administered five treatments with 5-FU and the other mice received four treatments with either saline or cisplatin. Flow cytometric analysis or fluorescence-activated cell sorting was performed 3 days after the last administration of an anticancer agent.

Flow Cytometric Analysis and Cell Sorting

Mice were euthanized and tumor tissues were excised, minced, and digested with Dispase II (Godo Shusei, Corp., Chiba, Japan) and collagenase (Wako, Osaka, Japan) with continuous shaking at 37°C. Single-cell suspensions of

tumor cells were prepared using a standard protocol.[16] Flow cytometric analysis was performed using a FACSCalibur (Becton Dickinson, Franklin Lakes, NJ), and cell sorting was performed using a FACSAria (Becton Dickinson). For the EGFP-high cell population, 5% of the most brightly fluorescing cells were sorted, and for the EGFP-low cell population, 5% of the least fluorescent cells were sorted. We used parental LLC or colon26 as negative controls.

In Vitro Colony Formation Analysis and *in Vivo* Tumor Initiation Analysis

Isolated cells were plated at a concentration of 500 cells per dish on 10-cm culture dishes and cultured in culture media with or without various doses of anticancer agents. For *in vivo* experiments, sorted cells were suspended in 100 μL of PBS with growth factor—reduced Matrigel (BD Biosciences, San Jose, CA) and injected subcutaneously into the mice. Tumorigenic ability was judged for 8 weeks after inoculation of tumor cells.

Immunohistochemistry

Dissected tissues were fixed in 4% paraformaldehyde and dehydrated in methanol. Fixed specimens were embedded in polyester wax (VWR International, Ltd., Lutterworth, UK) and cut into 7-μm sections as described.[24] The staining procedure of tissue sections was almost the same as previously reported.[25] Rabbit anti-GFP antibody (Invitrogen, Eugene, OR), rat anti-CD31 antibody (BD Biosciences), and mouse anti—α-SMA antibody (Sigma-Aldrich) were used for primary antibodies.

For the immunohistochemical analyses, biotin-conjugated goat anti-rabbit Ig (Dako, Carpinteria, CA) or biotin-conjugated goat anti-rat Ig (Invitrogen) was used as a secondary antibody. The Vectastain ABC Kit (Vector Laboratories, Burlingame, CA) was used to amplify the target antigen signal before the visualization of horseradish peroxidase by diaminobenzidine (Dojindo, Kumamoto, Japan). The 5-bromo-4-chloro-3-indoxyl phosphate and nitro blue tetrazolium chloride substrate system (Dako) was used for the visualization of alkaline phosphatase.

For the immunofluorescence analyses, Alexa Fluor 488—conjugated IgGs (Invitrogen) or streptavidin-allophycocyanin (APC) conjugate (BD Pharmingen, Franklin Lakes, NJ) was used as a second-step reagent. Images were acquired using a DFC 500 digital camera (Leica Microsystems, Nussloch, Germany) and processed with the Leica application suite and Adobe Photoshop CS2 software (Tokyo, Japan). All images shown are representative of three to six independent experiments.

Statistical Analysis

Results are expressed as the means ± SEM. The Student's *t*-test was used for statistical analysis except for the cumulative survival rate data, for which the log-rank test was used. Differences were considered statistically significant when the *P* value was less than 0.05.

Results

PSF1 Promoter Activity Does Not Affect Drug Sensitivity Directly in Colon26 and LLC Cells

We previously designated *PSF1*-promoter^{high} cancer cells as a population of CICs/CSCs in a mouse tumor cell allograft model because they had higher tumorigenic, invasive, and metastatic abilities compared with *PSF1*-promoter^{low} cancer cells and had an embryonic stem cell—specific immature gene signature.[16] First, we observed whether *PSF1*-promoter^{high} cancer cells showed drug resistance. We used colon cancer (colon26) cell lines and lung cancer (LLC) cell lines that stably expressed EGFP under the transcriptional control of the *PSF1*-promoter (colon26- and LLC-*PSF1p-EGFP*, respectively). In these cells, the intensity of EGFP is correlated with endogenous *PSF1* mRNA expression.[16] After inoculation of colon26- or LLC-*PSF1p-EGFP*, tumors were dissected and EGFP-high (5% most bright) or EGFP-low (5% least bright) cancer cells were sorted by a fluorescence-activated cell sorter (Figure 1, A and B). Sorted cells were cultured for 10 days in culture media containing various doses of 5-FU. As previously reported, EGFP-high cells formed significantly larger colonies, as well as a higher number of colonies, compared with EGFP-low cells for both colon26 and LLC cells (Figure 1, C and D). The number of colonies formed by both EGFP-high and EGFP-low cells decreased in a dose-dependent manner in the presence of 5-FU. At a glance, EGFP-low cells seemed to be more sensitive to 5-FU because colonies were not formed at higher doses of 5-FU. However, when the sensitivity to 5-FU was evaluated by the relative ratio of the number of colonies in the presence of 5-FU to that in the absence of 5-FU, no significant differences in sensitivity to 5-FU were observed between EGFP-high and EGFP-low cells (Figure 1, E and F). Therefore, we concluded that *PSF1*-promoter activity does not alter the drug sensitivity of the original cancers before 5-FU treatment, at least in colon26 and LLC cancer cells.

Expression Pattern of *PSF1* Promoter Activity in Remaining Cancer Cells after Treatment with Cancer Drug Is Different Depending on Cancer Cell Type

We next observed the level of *PSF1*-promoter activity in cancer cells after administration of a cancer drug in an allograft model using colon26- and LLC-*PSF1p-EGFP* cells. The administration of 5-FU *in vivo* had a marked cytoreductive effect in both tumors (Figure 2, A and B). However, there were obvious differences in EGFP fluorescence intensity of the residual cancer cells between colon26- and LLC-*PSF1p-EGFP* cells. In the case of colon26-*PSF1p-EGFP* cells, with 5-FU administration *in vivo* there was a marked

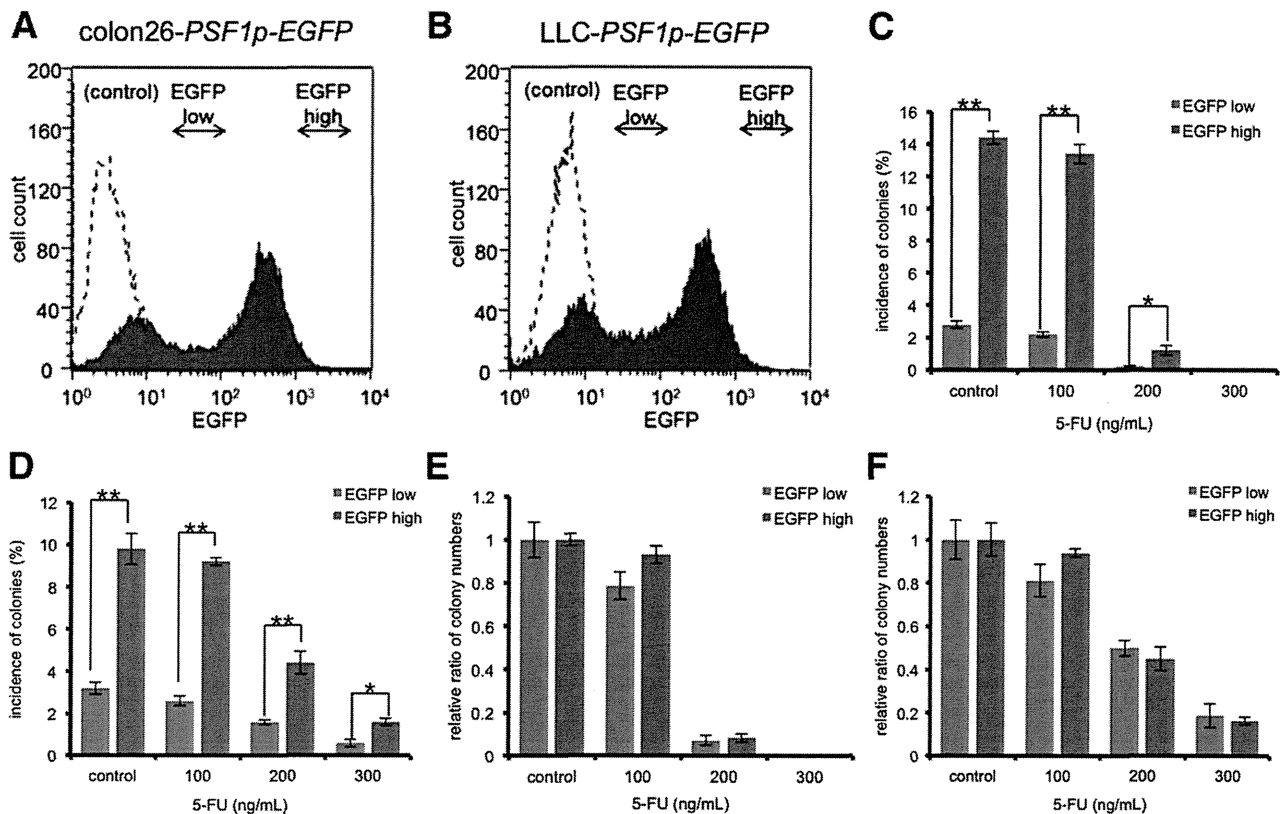

Figure 1 *PSF1*-promoter activity does not affect drug sensitivity directly in colon26 and LLC cells. **A:** Flow cytometric analysis of cells from tumor tissues. Tumors were derived from mice injected with colon26 (control: **dashed line**) or colon26-*PSF1p-EGFP* (**purple area**) cells (10^6 cells). **B:** Same experiment as described in **A** using LLC (control: **dashed line**) or LLC-*PSF1p-EGFP* (**purple area**) cells. **C** and **D:** Drug resistance analysis of sorted cells. Five hundred sorted cells as in **A** and **B**, respectively, were seeded onto 10-cm culture dishes and cultured in various dosages of 5-FU for 10 days. Colonies generated from different fractions were stained with Giemsa solution and assessed quantitatively. Data show the means ± SEM. $*P < 0.05$, $**P < 0.01$ ($n = 3$). **E** and **F:** Sensitivity to 5-FU. The relative ratio of the number of colonies in the presence of 5-FU to those in the absence of 5-FU obtained in experiments shown in **C** and **D**, respectively, was evaluated quantitatively. Data show the means ± SEM ($n = 3$).

reduction in the proportion of EGFP-high cells compared with the control group (Figure 2C). On the other hand, with LLC-*PSF1p-EGFP* cells, the proportion of EGFP-high cells increased after 5-FU administration in comparison with the control group (Figure 2D). Similar results were obtained with the administration of cisplatin (Supplemental Figure S1, A and B). These results showed a difference in the expression pattern of *PSF1*-promoter activity in residual cancer cells after cancer drug administration, depending on the cancer cell type.

PSF1-Promoter^{high} Cancer Cells Acquire Drug Resistance after Cancer Drug Administration

We previously reported that *PSF1*-promoter^{high} cancer cells had significantly higher tumorigenic activity than *PSF1*-promoter^{low} cancer cells.[16] We next assessed whether residual EGFP-high cancer cells after treatment with an anticancer drug (5-FU) in a tumor allograft model also would show tumor initiation activity and drug resistance in a second *in vitro* treatment with an anticancer drug. As shown in Figure 3A, LLC-*PSF1p-EGFP* cells were inoculated into mice and tumor-bearing mice were treated with 5-FU using the same schedule as described in Figure 2C. On day 18, tumors were dissected and two fractions of cancer cells (EGFP-low and EGFP-high cells) were sorted by a fluorescence-activated cell sorter as indicated (Figure 3A). Cancer cells (50, 100, or 1000) secondarily were inoculated into mice for observation of tumor initiation capacity. Moreover, cells were cultured in the presence or absence of 5-FU for 14 days and drug resistance was evaluated by calculating the number of colonies.

A smaller number of EGFP-high cells generated a secondary tumor more effectively than similar numbers of EGFP-low cells (Table 1). The difference in tumor initiation capacity between EGFP-low cells and EGFP-high cells was significant. When cultured in the presence or absence of 5-FU, EGFP-high cells formed significantly larger as well as a higher number of colonies than EGFP-low cells under all conditions (Figure 3B). In an evaluation of the sensitivity to 5-FU by the relative ratio of the number of colonies in the presence of 5-FU to those in the absence of 5-FU, EGFP-high cells showed significant resistance to 5-FU compared with EGFP-low cells (Figure 3C).

When EGFP-high or -low cells from tumors generated by colon26-*PSF1p-EGFP* cells were sorted on day 16 after

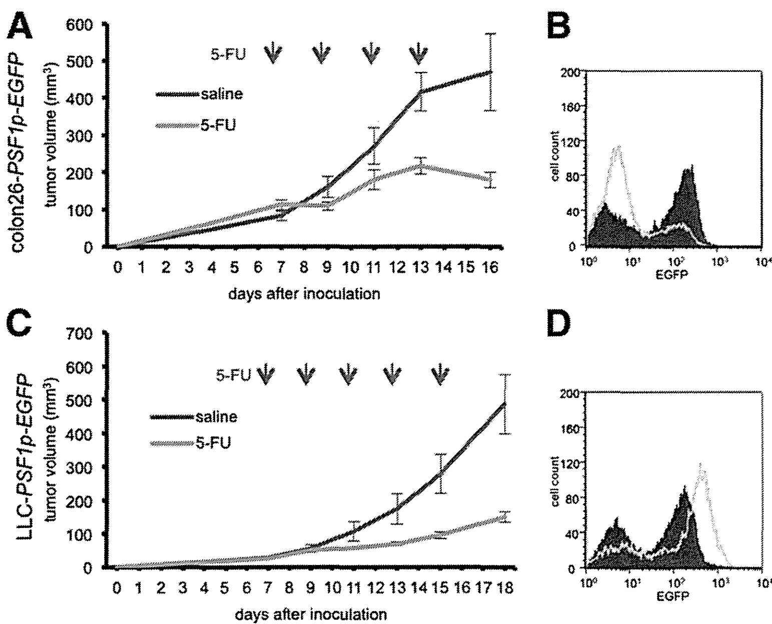

Figure 2 Expression pattern of *PSF1*-promoter activity in cancer cells that remain after treatment with cancer drug. **A:** Time course of tumor volume after 5-FU administration *in vivo*. 5-FU was administered to tumor-bearing mice inoculated by colon26-*PSF1p-EGFP* cells on days 7, 9, 11, and 13 as indicated by **red arrows**. Data show the means ± SEM ($n = 6$). **B:** Flow cytometric analysis of cells from tumor tissues on day 16 (as in **A**). Data obtained by flow cytometry in the saline (control) group (**purple area**) and the 5-FU–injected group (**green line**) represent the results of multiple experiments. **C:** Time course of tumor volume after 5-FU administration *in vivo*. 5-FU was administered to tumor-bearing mice inoculated by LLC-*PSF1p-EGFP* cells on days 7, 9, 11, 13, and 15 as indicated by **red arrows**. Data show the means ± SEM ($n = 7$). **D:** Flow cytometric analysis of cells from tumor tissues on day 18 (as in **C**). Data obtained by flow cytometry in the saline (control) group (**purple area**) and the 5-FU–injected group (**green line**) represent the results of multiple experiments.

administration of 5-FU using the same schedule as described in Figure 2 and cultured in the presence or absence of 5-FU, EGFP-high cells showed significant resistance to 5-FU compared with EGFP-low cells (Supplemental Figure S2, A–C) as observed in LLC tumors. EGFP-high cells and EGFP-low cells from non–5-FU–treated tumors did not show any differences in terms of drug resistance (Figure 1, E and F). This suggests that EGFP-high cells acquired drug resistance by the *in vivo* treatment with the cancer drug and became more malignant cancer cells, although their behavior was originally that of CICs/CSCs.

LLC Tumors, But Not Colon26 Tumors, Contain Abundant Mural Cell–Covered Mature Blood Vessels

In the case of an allograft model using colon26-*PSF1p-EGFP* cells, the proportion of EGFP-high cells decreased after 5-FU treatment as described earlier (Figure 2C), which was completely opposite of the result using LLC-*PSF1p-EGFP* cells (Figure 2D). These results suggest that the microenvironment in LLC tumors more effectively induced cancer cells to become drug resistant. Therefore, we next analyzed the characteristics of the tumor microenvironment, focusing especially on tumor vessels, because the vascular niche may be a key to the regulation of stemness of CSCs.[15,26]

In colon26 tumors the vascular density was high (Figure 4, A and C). However, most of the blood vessels were composed of endothelial cells alone and α-SMA–positive mural cell coverage of endothelial cells barely was observed. On the other hand, in case of LLC tumors, vascular density was not largely different from that in colon26 tumors, however, most of the blood vessels were covered with α-SMA–positive mural cells (Figure 4, B and D, and Supplemental Figure S3, A and B). The number of mural cells that covered blood vessels was four times higher in LLC tumors compared with colon26 tumors (Figure 4E). To investigate whether the distribution of mural cell–covered blood vessels was affected by 5-FU treatment, we observed blood vessel formation in colon26 tumors and LLC tumors on days 16 and 18, respectively, under the same schedule as described in Figure 2. The results suggested no remarkable differences in tumor blood vessels before and after 5-FU treatment (Supplemental Figure S3, C and D).

LLC-PSF1p-EGFP-High Cells Localize in the Mural Cell–Covered Blood Vessel Area

In the case of an allograft model using LLC-*PSF1p-EGFP* cells, the proportion of EGFP-high cells increased after 5-FU treatment as described earlier (Figure 2D). The high frequency of mural cell–covered blood vessels in LLC tumors was significantly different compared with that in colon26 tumors. It is possible that mural cell–covered blood vessels play a role in the induction of drug resistance in *PSF1p*-EGFP-high CICs/CSCs. If so, EGFP-high cells may localize near mural cell–covered blood vessels. To assess this, the tissue distribution of EGFP-high cells in tumors with or without 5-FU treatment was examined. With lower magnification, a dark brownish area where EGFP-high cells exist with high density was located in the marginal zone of the tumor mass regardless of 5-FU treatment (Figure 5, A and B). In this area, dark blue mural cell–covered blood vessels were observed frequently. By using higher magnification, it was apparent that EGFP-high cells were located near blood vessels in which endothelial cells were fully covered with α-SMA–positive mural cells (Figure 5, C and D). These results indicate that cancer cells expressing high levels of PSF1 are localized mainly near mature tumor

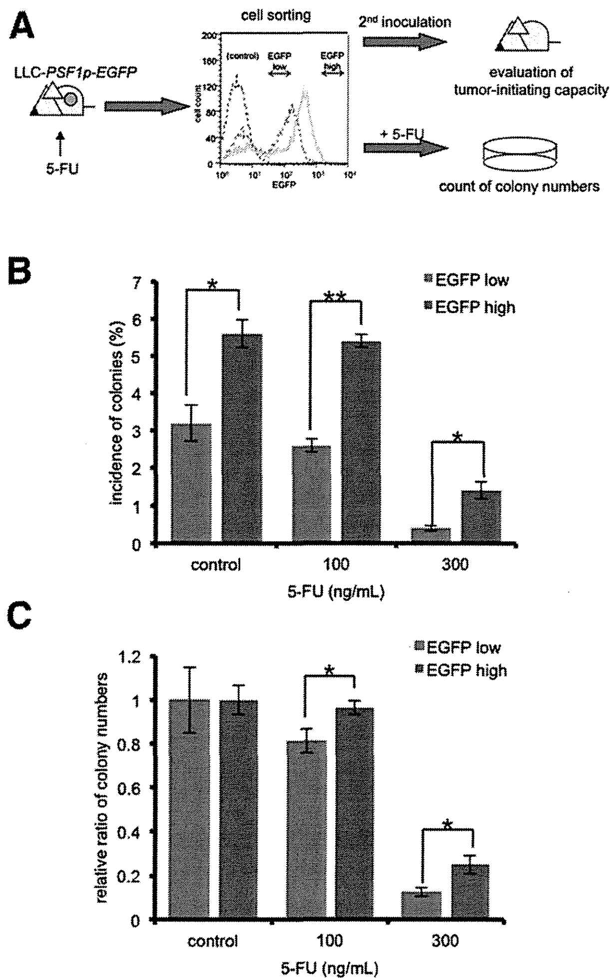

Figure 3 Acquisition of drug resistance after cancer drug administration. **A:** Analysis of the drug resistance capacity and tumor initiation capacity. Tumor-bearing mice by inoculation with LLC-*PSF1p-EGFP* cells were administered 5-FU as in Figure 2C. Tumor cells from the remaining tumor tissue were analyzed by flow cytometry and EGFP-high or EGFP-low cells were obtained. The **black line** shows LLC cells (no EGFP expression), the **red line** shows LLC-*PSF1p-EGFP* cells without 5-FU treatment, and the **green line** indicates LLC-*PSF1p-EGFP* cells treated with 5-FU *in vivo*. Cells from these two fractions were analyzed for *in vivo* tumorigenic activity and *in vitro* colony formation. **B:** Drug resistance analysis of residual cancer cells after 5-FU administration *in vivo*. Five hundred sorted cells as in **A** were seeded onto 10-cm culture dishes and cultured in various doses of 5-FU for 14 days. Colonies generated from different fractions were stained with Giemsa solution and assessed quantitatively. Data show the means $\pm$ SEM. $^*P < 0.05$, $^{**}P < 0.01$ ($n = 3$). **C:** Sensitivity to 5-FU. Relative ratio of the number of colonies in the presence of 5-FU to those in the absence of 5-FU obtained in experiment **B** was evaluated quantitatively. Data show the means $\pm$ SEM. $^*P < 0.05$ ($n = 3$).

blood vessels and that this microenvironment may contribute to cell survival and acquisition of drug resistance when tumors are exposed to anticancer agents.

Mature Blood Vessel Formation in Tumors Is Induced by Cancer Cells

Immunohistochemical analysis suggests that LLC cells induce mature blood vessel formation during tumorigenesis and that colon26 cancer cells cannot induce mature blood vessel formation abundantly. In summary, maturation of blood vessels appears to be induced depending on molecular cues from cancer cells, but not host cells. However, one of the most important concerns regarding our experimental systems is that the original hosts of the cancer cell lines used were different (ie, BALB/c mice for colon26 cells and C57BL/6 mice for LLC cells). Therefore, it is possible that the maturation of tumor blood vessels is affected by the strain of mouse. To test this possibility, a tumor transplantation model using nude mice for both colon26 and LLC cells was utilized.

As shown in Figure 6, α-SMA—positive mural cell—covered blood vessels barely were observed in colon26 tumors but were observed abundantly in LLC tumors (Figure 6, A and B). Similar to the original hosts, the number of blood vessels covered with mural cells was four times higher in LLC tumors compared with colon26 tumors (Supplemental Figure S4). This suggests that the maturation of blood vessels in tumors is induced depending on the tumor cells themselves. Moreover, when 5-FU was administered in this model using the same schedule as described in Figure 2, tumor growth effectively was inhibited in both tumors (Figure 6, C and D). In addition, as observed in the response of the original host allograft model, we confirmed that the proportion of EGFP-high cells decreased in colon26 tumors but increased in LLC tumors (Figure 6, E and F).

Finally, we analyzed whether the difference in the proportion of residual cancer cells expressing high levels of PSF1 (EGFP-high cells) would affect therapeutic performance such as prolonged survival. Survival periods of nude mice bearing colon26- or LLC-*PSF1p-EGFP* cells were observed after 5-FU administration. Survival of mice bearing colon26 tumors, in which the EGFP-high cell population was reduced dramatically by 5-FU treatment, was prolonged significantly compared with mice that received no medication (Figure 6G). On the other hand, the mice bearing an LLC tumor, in which EGFP-high cells resided after treatment with 5-FU, did not survive longer than mice that received no medication (Figure 6H). These results indicate that the existence of residual cancer cells

Table 1 Tumor Initiation Rate in Serial Transplantation

LLC-*PSF1p-EGFP* cells	EGFP low	EGFP high
1000 cells	100% ($n = 5$)	100% ($n = 5$)
100 cells	70% ($n = 10$)	100% ($n = 10$)
50 cells	80% $\pm$ 6.7%* ($n = 10 \times 3$)	100% $\pm$ 0% ($n = 10 \times 3$)

A small number of sorted cells as indicated were inoculated subcutaneously into mice and tumor formation was observed until 8 weeks after tumor cell inoculation. Quantitative evaluation was conducted using 50 sorted cells. Experiments were performed three times with similar results. Data show the means $\pm$ SEM. Statistic evaluation was performed between data of 50 cells. $^*P < 0.05$ ($n = 10$).

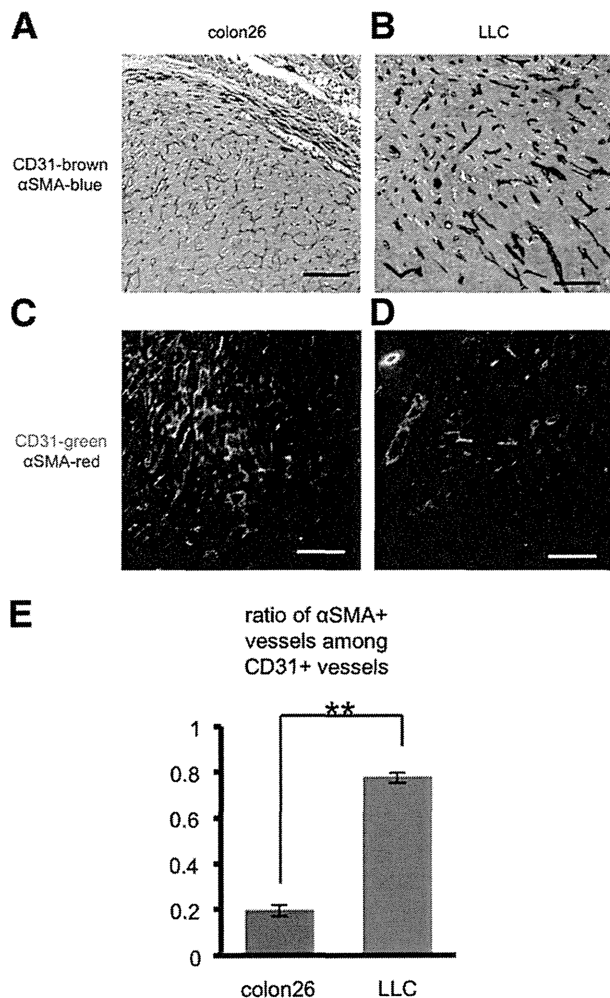

Figure 4 Immunohistochemical and immunofluorescence analyses of tumor vessels. **A** and **B**: Sections from colon26 (**A**) and LLC (**B**) tumors were double-stained with anti-CD31 antibody (brown) and anti–α-SMA antibody (blue). Scale bars: 200 μm. **C** and **D**: Sections from colon26 (**C**) and LLC (**D**) tumors were double-stained with anti-CD31 antibody (green) and anti–α-SMA antibody (red). Scale bars: 200 μm. **E**: The ratio of α-SMA–positive mural cell–covered blood vessels to all CD31-positive tumor vessels. Data are means ± SEM from five random fields. $^{**}P < 0.01$.

expressing high levels of PSF1 might be an important factor affecting prolonged survival.

Discussion

In this study, we analyzed the relationship between the tumor microenvironment and cancer cell malignancy using two different tumor cell types. The colon26 tumors produced abundant blood vessels; however, there were few mural cell–covered mature blood vessels. On the other hand, LLC tumors contained α-SMA–positive mural cell–covered mature blood vessels with high frequency. In normal organs, it was reported that the stem cell population self-renews in vascular areas.[27,28] It is possible that CICs/CSCs also localize in perivascular areas for self-renewal. Usually, blood vessels in normal organs are mural cell–covered mature blood vessels. Therefore, it is reasonable that mature blood vessels function as the vascular niche for stem cells. This suggests that a cancer microenvironment composed of abundant mature blood vessels, as in LLC tumors, may support the stemness of CSCs.

By using methods to identify malignant CICs by means of higher transcriptional activity of the *Psf1* gene, we found that drug resistance of CICs in original LLC or colon26 tumors was not largely different compared with *PSF1*-promoter^{low} cancer cells. However, after administration of an anticancer drug, residual *PSF1*-promoter^{high} CICs acquired drug resistance. In particular, the proportion of *PSF1*-promoter^{high} CICs increased in LLC tumors in which mature blood vessels were highly observed. Therefore, these results suggest that the microenvironment supports acquisition of drug resistance in cancer cells after anticancer drug administration and that mature blood vessels may be involved in this event.

The number of colonies derived from EGFP-high cells sorted from tumors decreased after *in vivo* 5-FU treatment (Figure 3B) compared with the number of colonies generated by cells of nontreated tumors (Figure 1D). Cells used in the experiment shown in Figure 3B already were exposed to 5-FU *in vivo*; thus, the condition of cells in Figure 1D is different from that of cells in Figure 3B. *PSF1*-promoter activity also may correlate with the cell cycle, and cycling cells are more affected by 5-FU *in vivo*. Here, it is emphasized that drug resistance by EGFP-high cells is induced after *in vivo* anticancer drug treatment.

Preliminary results suggest that among 5-FU–resistant genes, thymidylate synthase was up-regulated slightly in EGFP-high LLC cells after *in vivo* treatment with 5-FU compared with EGFP-low cells. Moreover, ABCB1 (MDR1) expression was up-regulated slightly without statistical significance. In terms of drug resistance, further precise analysis is required.

Recently, one report suggested that the population of CSCs in a tumor increased after treatment with an angiogenesis inhibitor.[29] The report suggested that hypoxia induced by the regression of blood vessels by an angiogenesis inhibitor activated the AKT signaling pathway in CSCs, resulting in the proliferation of CSCs. It is widely accepted that angiogenesis inhibitors normalize tumor blood vessels, resulting in effective induction of drug delivery into the parenchyma of a malignant tumor.[30] We previously showed that mural cell coverage of endothelial cells in tumors is induced by treatment with angiogenesis inhibitors.[31] In our present work, drug resistance of CICs was promoted effectively in tumors in which mature blood vessels abundantly were observed. Taken together, this suggests that expansion of CSCs after angiogenesis inhibitor treatment is associated with maturation of tumor blood vessels. In addition, it previously was reported that invasion of cancer cells was enhanced after angiogenesis inhibitor treatment in tumors.[32,33] To prevent normal blood vessels from damage, excessive amounts of angiogenesis inhibitor cannot be used. Because of this situation, mature blood vessels in tumors can survive. Considering that mature blood vessels may educate

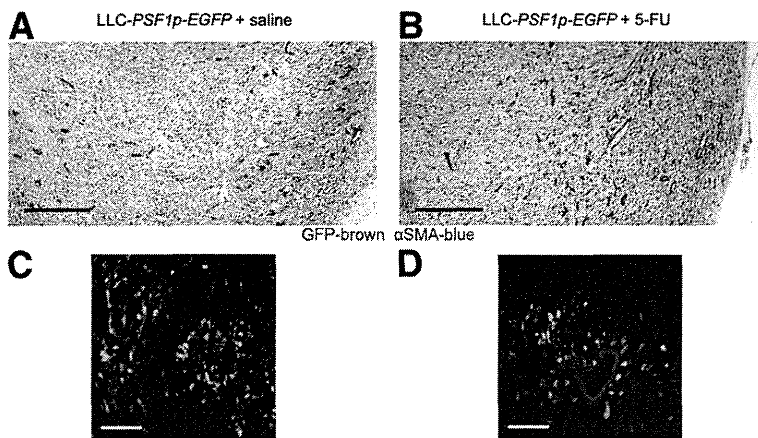

Figure 5 Localization of cancer cells with higher *PSF1*-promoter activity before and after 5-FU administration. **A** and **B**: LLC-*PSF1p-EGFP* cells subcutaneously inoculated into mice. Sections from tumor on day 18 as in Figure 2C with (**B**) or without (**A**) administration of 5-FU were double-stained with anti-GFP antibody (brown) and anti–α-SMA antibody (blue). Scale bar = 500 μm. **C** and **D**: Sections of tumor as in **A** or **B**, respectively, were stained with anti-GFP antibody (green), anti–α-SMA antibody (red), and anti-CD31 antibody (blue). Scale bars: 100 μm.

cancer cells to become aggressive cancer cells, the molecular mechanism of how blood vessels in tumors become mature should be elucidated.

In our present work, to clarify the involvement of mature blood vessels in the acquisition of malignant features by cancer cells, such as drug resistance, we tried to inhibit the transforming growth factor-β pathway. Because it has been reported that inhibition of the transforming growth factor-β signal suppressed mural cell–endothelial cell attachment,[34] we pursued this line of work to suppress mural cell coverage on endothelial cells in LLC tumors and analyzed whether the proportion of *PSF1p-EGFP*–high CICs decreased with 5-FU treatment. However, inhibition of the transforming growth factor-β signal suppressed angiogenesis itself and

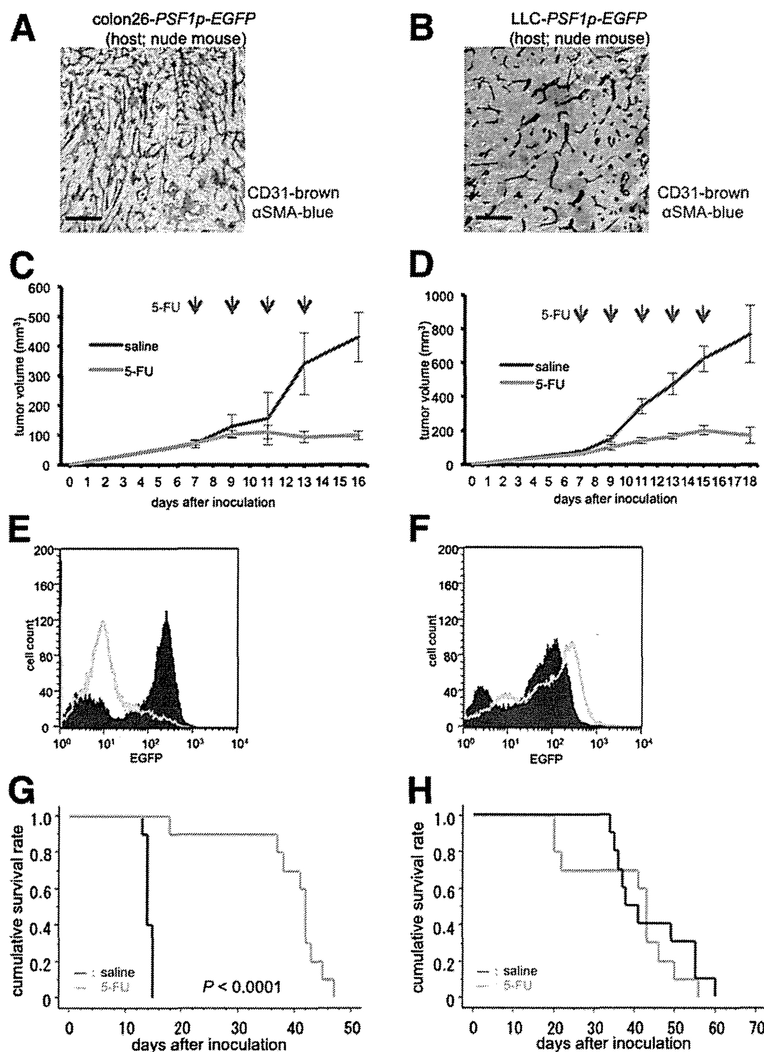

Figure 6 Relationship of maturation of blood vessels and survival of tumor-bearing mice after treatment with anticancer drug. **A** and **B**: Immunohistochemical staining of tumor sections derived from tumor inoculated by colon26- (**A**) and LLC- (**B**) *PSF1p-EGFP* cells into nude mice. Sections were stained with anti-CD31 antibody (brown) and anti–α-SMA antibody (blue). Scale bars: 200 μm. **C** and **D**: Time course of tumor volume after 5-FU administration *in vivo* using nude mice as in **A** or **B**, respectively. **Red arrows** indicate the date of 5-FU injection. **E** and **F**: Flow cytometric analysis of cells from tumor tissues on day 16 (as in **C**) or on day 18 (as in **D**), respectively. Data obtained by flow cytometry in the saline (control) group (**purple area**) and the 5-FU–injected group (**green line**) represent the results of multiple experiments. **G** and **H**: Kaplan-Meier curve of nude mice bearing colon26 tumors as in **C** or LLC tumors as in **D**, respectively, after 5-FU administration (n = 10 for each group).

tumor growth was inhibited, but inhibition of blood vessel maturation was not observed clearly in our studies.

As to other possible ways to inhibit the maturation of blood vessels in tumors, inhibition of the platelet-derived growth factor signal has been considered because of its effect on recruitment of mural cells near endothelial cells.[35] However, inhibition of the platelet-derived growth factor signal also decreased interstitial hypertension in tumor parenchyma for improvement of drug delivery,[36] suggesting that clear conclusions on inhibition of the maturation of blood vessels could not be drawn through the use of a platelet-derived growth factor inhibitor. Therefore, the specific molecular mechanism regulating the maturation of blood vessels, especially in LLC-type tumors, should be elucidated and used for inhibition of tumor blood vessel maturation.

Results of the present study suggest that cells composing the tumor microenvironment support the acquisition of drug resistance in CICs after cancer drug administration. How stromal cells in the tumor microenvironment change their characteristics to provide cancer cells with malignancy is completely unknown. We previously reported that exogenous molecular cues stimulate stromal cells to alter the cell fate of co-cultured hematopoietic stem cells.[37] When OP9 osteoblastic stromal cells were stimulated with epidermal growth factor or activated by transfection with the constitutive active form of erbB2 to exclude the direct effect of epidermal growth factor on hematopoietic stem cells, self-renewal of co-cultured hematopoietic stem cells was induced. On the other hand, when OP9 cells were stimulated with basic fibroblast growth factor, co-cultured hematopoietic stem cells quickly differentiated. Similarly, when endothelial cells were used as stromal cells and activated with the constitutive active form of AKT, self-renewal of co-cultured hematopoietic stem cells was induced.[38] On the other hand, when c-raf was transfected and the extracellular signal-regulated kinase pathway was activated in endothelial cells, differentiation of co-cultured hematopoietic stem cells was induced. Therefore, these findings suggest that different molecular cues that affect the same stromal cells alter behavior of the neighboring stem cell population via factors derived from stromal cells. In summary, niche cells of CICs/CSCs in the cancer microenvironment may intrinsically change their characteristics after cancer drug treatment or be affected indirectly by other cell components and may provide CICs/CSCs with acquisition of drug resistance. Further precise analysis will be necessary to investigate what kind of molecular mechanism underlies the induction of malignancy in CICs/CSCs.

Finally, we would like to emphasize that the tumor cell transplantation model reflects only a part of actual cancer tissue in patients. Tumor tissue in patients may comprise heterogeneous CICs/CSCs. Moreover, niche cells are not homogeneous. Therefore, the response to a cancer drug in the tumor environment varies even within the same patient. We need to clarify the central principle to support the malignant features of CICs/CSCs for the development of a new strategy to inhibit tumor growth.

Acknowledgments

We thank Keisho Fukuhara and Noriko Fujimoto for general assistance.

Supplemental Data

Supplemental material for this article can be found at *http://dx.doi.org/10.1016/j.ajpath.2013.01.019.*

References

1. Hanahan D, Weinberg RA: Hallmarks of cancer: the next generation. Cell 2011, 144:646–674
2. Gupta PB, Chaffer CL, Weinberg RA: Cancer stem cells: mirage or reality? Nat Med 2009, 15:1010–1012
3. Ben-Porath I, Thomson MW, Carey VJ, Ge R, Bell GW, Regev A, Weinberg RA: An embryonic stem cell-like gene expression signature in poorly differentiated aggressive human tumors. Nat Genet 2008, 40:499–507
4. Wong DJ, Liu H, Ridky TW, Cassarino D, Segal E, Chang HY: Module map of stem cell genes guides creation of epithelial cancer stem cells. Cell Stem Cell 2008, 2:333–344
5. Somervaille TC, Matheny CJ, Spencer GJ, Iwasaki M, Rinn JL, Witten DM, Chang HY, Shurtleff SA, Downing JR, Cleary ML: Hierarchical maintenance of MLL myeloid leukemia stem cells employs a transcriptional program shared with embryonic rather than adult stem cells. Cell Stem Cell 2009, 4:129–140
6. Bao S, Wu Q, McLendon RE, Hao Y, Shi Q, Hjelmeland AB, Dewhirst MW, Bigner DD, Rich JN: Glioma stem cells promote radioresistance by preferential activation of the DNA damage response. Nature 2006, 444:756–760
7. Frank NY, Schatton T, Frank MH: The therapeutic promise of the cancer stem cell concept. J Clin Invest 2010, 120:41–50
8. Loebinger MR, Giangreco A, Groot KR, Prichard L, Allen K, Simpson C, Bazley L, Navani N, Tibrewal S, Davies D, Janes SM: Squamous cell cancers contain a side population of stem-like cells that are made chemosensitive by ABC transporter blockade. Br J Cancer 2008, 98:380–387
9. Miletti-González KE, Chen S, Muthukumaran N, Saglimbeni GN, Wu X, Yang J, Apolito K, Shih WJ, Hait WN, Rodríguez-Rodríguez L: The CD44 receptor interacts with P-glycoprotein to promote cell migration and invasion in cancer. Cancer Res 2005, 65:6660–6667
10. Angelastro JM, Lamé MW: Overexpression of CD133 promotes drug resistance in C6 glioma cells. Mol Cancer Res 2010, 8:1105–1115
11. Cabarcas SM, Mathews LA, Farrar WL: The cancer stem cell niche—there goes the neighborhood? Int J Cancer 2011, 129:2315–2327
12. Kiel MJ, Morrison SJ: Maintaining hematopoietic stem cells in the vascular niche. Immunity 2006, 25:862–864
13. Mikkola HK, Orkin SH: The journey of developing hematopoietic stem cells. Development 2006, 133:3733–3744
14. Adams GB, Scadden DT: The hematopoietic stem cell in its place. Nat Immunol 2006, 7:333–337
15. Calabrese C, Poppleton H, Kocak M, Hogg TL, Fuller C, Hamner B, Oh EY, Gaber MW, Finklestein D, Allen M, Frank A, Bayazitov IT, Zakharenko SS, Gajjar A, Davidoff A, Gilbertson RJ: A perivascular niche for brain tumor stem cells. Cancer Cell 2007, 11:69–82
16. Nagahama Y, Ueno M, Miyamoto S, Morii E, Minami T, Mochizuki N, Saya H, Takakura N: PSF1, a DNA replication factor

expressed widely in stem and progenitor cells, drives tumorigenic and metastatic properties. Cancer Res 2010, 70:1215–1224

17. Beck B, Driessens G, Goossens S, Youssef KK, Kuchnio A, Caauwe A, Sotiropoulou PA, Loges S, Lapouge G, Candi A, Mascre G, Drogat B, Dekoninck S, Haigh JJ, Carmeliet P, Blanpain C: A vascular niche and a VEGF-Nrp1 loop regulate the initiation and stemness of skin tumours. Nature 2011, 478:399–403
18. Vermeulen L, De Sousa E, Melo F, van der Heijden M, Cameron K, de Jong JH, Borovski T, Tuynman JB, Todaro M, Merz C, Rodermond H, Sprick MR, Kemper K, Richel DJ, Stassi G, Medema JP: Wnt activity defines colon cancer stem cells and is regulated by the microenvironment. Nat Cell Biol 2010, 12:468–476
19. Takayama Y, Kamimura Y, Okawa M, Muramatsu S, Sugino A, Araki H: GINS, a novel multiprotein complex required for chromosomal DNA replication in budding yeast. Genes Dev 2003, 17:1153–1165
20. Kamada K, Kubota Y, Arata T, Shindo Y, Hanaoka F: Structure of the human GINS complex and its assembly and functional interface in replication initiation. Nat Struct Mol Biol 2007, 14:388–396
21. Ueno M, Itoh M, Kong L, Sugihara K, Asano M, Takakura N: PSF1 is essential for early embryogenesis in mice. Mol Cell Biol 2005, 25:10528–10532
22. Han Y, Ueno M, Nagahama Y, Takakura N: Identification and characterization of stem cell-specific transcription of PSF1 in spermatogenesis. Biochem Biophys Res Commun 2009, 380:609–613
23. Ueno M, Itoh M, Sugihara K, Asano M, Takakura N: Both alleles of PSF1 are required for maintenance of pool size of immature hematopoietic cells and acute bone marrow regeneration. Blood 2009, 113:555–562
24. Takakura N, Watanabe T, Suenobu S, Yamada Y, Noda T, Ito Y, Satake M, Suda T: A role for hematopoietic stem cells in promoting angiogenesis. Cell 2000, 102:199–209
25. Takakura N, Huang XL, Naruse T, Hamaguchi I, Dumont DJ, Yancopoulos GD, Suda T: Critical role of the TIE2 endothelial cell receptor in the development of definitive hematopoiesis. Immunity 1998, 9:677–686
26. Wang R, Chadalavada K, Wilshire J, Kowalik U, Hovinga KE, Geber A, Fligelman B, Leversha M, Brennan C, Tabar V: Glioblastoma stem-like cells give rise to tumour endothelium. Nature 2010, 468:829–833
27. Ding L, Saunders TL, Enikolopov G, Morrison SJ: Endothelial and perivascular cells maintain haematopoietic stem cells. Nature 2012, 481:457–462
28. Bautch VL: Stem cells and the vasculature. Nat Med 2011, 17:1437–1443
29. Conley SJ, Gheordunescu E, Kakarala P, Newman B, Korkaya H, Heath AN, Clouthier SG, Wicha MS: Antiangiogenic agents increase breast cancer stem cells via the generation of tumor hypoxia. Proc Natl Acad Sci U S A 2012, 109:2784–2789
30. Jain RK: Normalization of tumor vasculature: an emerging concept in antiangiogenic therapy. Science 2005, 307:58–62
31. Naito H, Takara K, Wakabayashi T, Kawahara H, Kidoya H, Takakura N: Changes in blood vessel maturation in the fibrous cap of the tumor rim. Cancer Sci 2012, 103:433–438
32. Ebos JM, Lee CR, Cruz-Munoz W, Bjarnason GA, Christensen JG, Kerbel RS: Accelerated metastasis after short-term treatment with a potent inhibitor of tumor angiogenesis. Cancer Cell 2009, 15:232–239
33. Pàez-Ribes M, Allen E, Hudock J, Takeda T, Okuyama H, Viñals F, Inoue M, Bergers G, Hanahan D, Casanovas O: Antiangiogenic therapy elicits malignant progression of tumors to increased local invasion and distant metastasis. Cancer Cell 2009, 15:220–231
34. Kano MR, Bae Y, Iwata C, Morishita Y, Yashiro M, Oka M, Fujii T, Komuro A, Kiyono K, Kaminishi M, Hirakawa K, Ouchi Y, Nishiyama N, Kataoka K, Miyazono K: Improvement of cancer-targeting therapy, using nanocarriers for intractable solid tumors by inhibition of TGF-beta signaling. Proc Natl Acad Sci U S A 2007, 104:3460–3465
35. Lindblom P, Gerhardt H, Liebner S, Abramsson A, Enge M, Hellstrom M, Backstrom G, Fredriksson S, Landegren U, Nystrom HC, Bergstrom G, Dejana E, Ostman A, Lindahl P, Betsholtz C: Endothelial PDGF-B retention is required for proper investment of pericytes in the microvessel wall. Genes Dev 2003, 17:1835–1840
36. Pietras K, Ostman A, Sjöquist M, Buchdunger E, Reed RK, Heldin CH, Rubin K: Inhibition of platelet-derived growth factor receptors reduces interstitial hypertension and increases transcapillary transport in tumors. Cancer Res 2001, 61:2929–2934
37. Takakura N, Kodama H, Nishikawa S, Nishikawa S: Preferential proliferation of murine colony-forming units in culture in a chemically defined condition with a macrophage colony-stimulating factor-negative stromal cell clone. J Exp Med 1996, 184:2301–2309
38. Kobayashi H, Butler JM, O'Donnell R, Kobayashi M, Ding BS, Bonner B, Chiu VK, Nolan DJ, Shido K, Benjamin L, Rafii S: Angiocrine factors from Akt-activated endothelial cells balance self-renewal and differentiation of haematopoietic stem cells. Nat Cell Biol 2010, 12:1046–1056

The American Journal of Pathology, Vol. 182, No. 5, May 2013

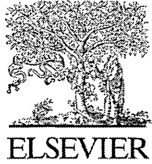

ELSEVIER

The American Journal of
PATHOLOGY

ajp.amjpathol.org

TUMORIGENESIS AND NEOPLASTIC PROGRESSION

Galectin-3 Accelerates M2 Macrophage Infiltration and Angiogenesis in Tumors

Weizhen Jia,* Hiroyasu Kidoya,* Daishi Yamakawa,* Hisamichi Naito,* and Nobuyuki Takakura*†

From the Department of Signal Transduction, Research Institute for Microbial Diseases, Osaka University, Osaka; and Japan Science and Technology Agency (JST),† K's Gobancho, Tokyo, Japan*

Accepted for publication January 10, 2013.

Address correspondence to Nobuyuki Takakura, M.D., Ph.D., Department of Signal Transduction, Research Institute for Microbial Diseases, Osaka University, 3-1 Yamada-oka, Suita, Osaka 565-0871, Japan. E-mail: ntakaku@biken.osaka-u.ac.jp.

It is widely accepted that robust invasion of tumor-associated macrophages resembling M2 macrophage correlates with disease aggressiveness by affecting cancer cell invasion, metastasis, and angiogenesis. Many chemokines that induce migration of macrophages have been identified during inflammatory responses; however, further precise analysis of macrophage migration in the tumor microenvironment is required. Here, we analyzed the function of galectin-3 (Gal-3; gene *LGALS3*, alias *Gal3*) for macrophage chemotaxis using *Gal3*$^{-/-}$ mice as hosts, and a tumor allograft model. We engineered a concentration gradient of Gal-3 produced by the tumor. In this model, we found that macrophage infiltration was enhanced in tumors developing in these *Gal3*$^{-/-}$ mice relative to the *Gal3*$^{+/+}$ animals. This was accompanied by enhanced tumor angiogenesis and tumor growth in *Gal3*$^{-/-}$ mice. We found that macrophages of the M2 phenotype were dominant in infiltrates in the *Gal3*$^{-/-}$ mice and that they expressed only low levels of Gal-3. *Gal3* knockdown by siRNA in macrophages resulted in enhanced chemotaxis. These data suggest that M2-like macrophages migrate into the tumor along a Gal-3 gradient and that high-level Gal-3 expression in the tumor results in acceleration of angiogenesis and tumor growth. Therefore, Gal-3 could be a potential target for the development of new treatments to inhibit tumor growth. *(Am J Pathol 2013, 182: 1821–1831; http://dx.doi.org/10.1016/j.ajpath.2013.01.017)*

Neovascularization is an indispensable event for tissue/organ development. New blood vessel formation observed under pathologic and physiological conditions occurs mainly by sprouting angiogenesis (ie, the development of a new branch from pre-existing vessels).[1] In sprouting angiogenesis, proangiogenic factors released from hypoxic regions or sites of inflammation directly induce migration and proliferation of endothelial cells (ECs). Moreover, nonvascular cells infiltrating into the region produce angiogenic factors that induce angiogenesis indirectly.[2,3]

We previously reported that hematopoietic stem/progenitor cells and CD11b^{low} immature myeloid cells/monocytes induce angiogenesis and maturation of newly developed blood vessels by secretion of angiopoietin-1, a ligand for receptor tyrosine kinase Tie2 expressed on ECs.[4,5] In addition, it is widely accepted that matrix metalloproteinase derived from mast cells, neutrophils, and macrophages promotes angiogenesis by matrix remodeling, and that vascular endothelial growth factor secreted by these cell populations also regulates angiogenesis.[6] Among hematopoietic lineages, the relationships of macrophages to angiogenesis have been examined extensively and crucial roles, especially of tumor-associated macrophages and Tie2-expressing macrophages, for tumor angiogenesis have been reported.[7,8]

Monocyte chemoattractant protein-1 (also known as chemokine ligand 2) and colony-stimulating factor-1 (also known as macrophage-colony-stimulating factor) are well-known chemoattractants for monocytes/macrophages, but other factors such as placental growth factor, chemokine ligand 3 (macrophage inflammatory protein 1), chemokine ligand 4, chemokine ligand 5 (regulated on activation normal T-cell expressed and secreted), and vascular endothelial growth factor also have been reported to act this way.[9,10] Therefore, further precise investigation is required to identify the molecules inducing monocyte/macrophage migration.

Here, we investigated relationships among galactose-binding lectin-3 (alias galectin-3; Gal-3), monocytes/macrophages, and

Supported by a Grant-in-Aid for Scientific Research from the Ministry of Education, Culture, Sports, Science, and Technology and the Japan Society for the Promotion of Science.

Copyright © 2013 American Society for Investigative Pathology.
Published by Elsevier Inc. All rights reserved.
http://dx.doi.org/10.1016/j.ajpath.2013.01.017

angiogenesis. Galectins are a family of lectins containing conserved carbohydrate-recognition domains specific for β-galactoside.[11] Gal-3 is a 32-kDa protein containing one carbohydrate-recognition domain and an N-terminal nonlectin domain. Different functions for Gal-3 in development, immune reactions, and tumorigenesis have been reported.[12] In macrophages, expression of Mac-2 (another name for Gal-3) has been reported. Published evidence suggests that Gal-3 may influence the migration of monocytes/macrophages.[13] However, the precise function of Gal-3 for monocyte/macrophage migration in the context of angiogenesis has not been clarified.

Thus far, although it has been reported that the mobility of ECs is enhanced by scaffolding generated through the binding of Gal-3 to integrin, *in vivo* roles of Gal-3 in angiogenesis have been minimally investigated. Because it has been reported that tumor cells express abundant Gal-3[12,14] and tumor angiogenesis is one available model for investigating Gal-3 function, we examined the role of Gal-3 in angiogenesis using *Gal3*-deficient mice.

Materials and Methods

Animals

C57BL/6 mice (7 to 8 weeks of age) were purchased from Japan SLC (Shizuoka, Japan). *Gal3* knockout (KO) mice (7 to 8 weeks of age) were generated as previously described.[15] Animals were housed in environmentally controlled rooms of the animal experimentation facility at Osaka University. All experiments were performed in accordance with the guidelines of Osaka University Committee for Animal and Recombinant DNA Experiments. Mice were handled and maintained according to Osaka University guidelines for animal experimentation.

Cell Culture

Cell lines, including B16 (mouse melanoma), mouse Lewis lung carcinoma (LLC), and J774 (murine macrophage), were purchased from the Riken cell bank (Tsukuba, Japan). The B16 and LLC cell lines were cultured in Dulbecco's modified Eagle's medium (Sigma, St. Louis, MO) supplemented with 10% fetal bovine serum and 1% penicillin/streptomycin. The J774 cell line was cultured in Dulbecco's modified Eagle's medium supplemented with 10% fetal bovine serum, 1% penicillin/streptomycin, and 2 mol/L L-glutamine (Gibco, Life Technologies, St. Paul, Brazil). Single-cell suspensions from tumor tissue were produced as previously described.[16] Murine bone marrow–derived macrophages ($CD45^{high}$ $CD11b^{high}$ $F4/80^{high}$) were isolated and prepared as previously described[16] and were cultured in RPMI-1640 (Sigma) supplemented with 10% fetal bovine serum, 1% penicillin/streptomycin, 2 mmol/L L-glutamine, and 50-ng/mL murine M-colony-stimulating factor (PeproTech, Rocky Hill, NJ). These bone marrow–derived macrophages were maintained for 7 days in a CO_2 incubator.

Quantitative Real-Time RT-PCR

Total RNA was extracted from cells and tumor tissues using RNeasy-plus mini kits (Qiagen, Hilden, Germany) and was reverse-transcribed using the PrimeScript RT reagent Kit (Takara, Kyoto, Japan) according to the manufacturer's protocol. Real-time PCR analysis was performed using Platinum SYBR Green qPCR SuperMix-UDC (Invitrogen, Carlsbad, CA) and an Mx3000p QPCR System (Stratagene, La Jolla, CA). The baseline and threshold were adjusted according to the manufacturer's instructions. The level of the target gene expression was normalized to that of glyceraldehyde-3-phosphate dehydrogenase in each sample. We used the following primer sets for mouse genes: 5′-CCACGTCGTAGCAAACCACCA-3′ (forward) and 5′-AGGAGCACGTAGTCGGGGCA-3′ (reverse) for tumor necrosis factor-α, 5′-TCCTCTCTGCAAGAGACTTCC-ATCC-3′ (forward) and 5′-GGGAAGGCCGTGGTTGT-CACC-3′ (reverse) for *IL6*, 5′-AGGCTCATCCAGAG-CCCGGAG-3′ (forward) and 5′-AGGGTGGTGCGGCTG-GACTT-3′ (reverse) for inducible nitric oxide synthase, 5′-TCGGTGGACTGTGGACGAGCA-3′ (forward) and 5′-TCCCGCCTTTCGTCCTGGCA-3′ (reverse) for macrophage mannose receptor 1 (MRC1), 5′-CCCCAGGCAGAGAA-GCATGGC-3′ (forward) and 5′-GGGGAGAAATCGATG-ACAGCGCC-3′ (reverse) for *IL10*, 5′-TCAGCCAGATG-CAGTTAACGCCC-3′ (forward) and 5′-GCTTCTTTGGG-ACACCTGCTGCT-3′ (reverse) for monocyte chemoattractant protein-1, 5′-TGCCCTATGACCTGCCCTT-3′ (forward) and 5′-TCCTGCTTCGTGTTACACACAA-3′ (reverse) for *Gal3* and, finally, 5′-TGGCAAAGTGGAGATTGTTGCC-3′ (forward) and 5′-AAGATGGTGATGGGCTTCCCG-3′ (reverse) for glyceraldehyde-3-phosphate dehydrogenase (*Gapdh*).

Western Blotting Analysis

Methods for Western blotting were as previously described.[17] Briefly, lysates from whole cells were resolved in SDS-PAGE. Proteins electrophoretically separated using 12.5% SDS-PAGE gels were transferred to nylon membranes (Amersham, Buckinghamshire, UK) by a wet blotting procedure and incubated with the following antibodies: rat anti-mouse Gal-3/MAC-2 (Cedarlane, Ontario, Canada); and anti-mouse glyceraldehyde-3-phosphate dehydrogenase (Millipore, Temecula, CA). Proteins were detected with horseradish-peroxidase–conjugated goat anti-rat IgG, goat anti-mouse IgG (Jackson Laboratories, Bar Harbor, ME) secondary antibodies and ECL reagents (Amersham). The blots were scanned with an imaging densitometer LAS-3000 mini (Fujifilm, Tokyo, Japan).

RNA Interference

siRNA specific to mouse Gal-3 and negative control siRNA were purchased from Sigma and transfected into J774 cells using Lipofectamine 2000 (Invitrogen) according to the